Appendix for Miles Herkenham 2008 BSC
Section on Functional Neuroanatomy, NIMH

Table of Contents

Appendix

Behavioral Studies
NFkB1-/- (p50 KO) mouse from JAX (129/B6 background)

We conducted extensive follow-up work after publishing the study showing the reduced-anxiety phenotype of the p50 KO mouse (2). Additional studies employed were the resident-intruder task, acoustic startle, and fear conditioning with tests for cue- and context-dependent recall. The tests were selected on the basis of the apparent phenotype already characterized. The studies were done in collaboration with Heather Caldwell, an expert in social behavior in W. Scott Young's lab, and Alexei Morozov, an expert in automated startle and fear conditioning tasks, in the Laboratory of Molecular Pathophysiology.

Acoustic Startle

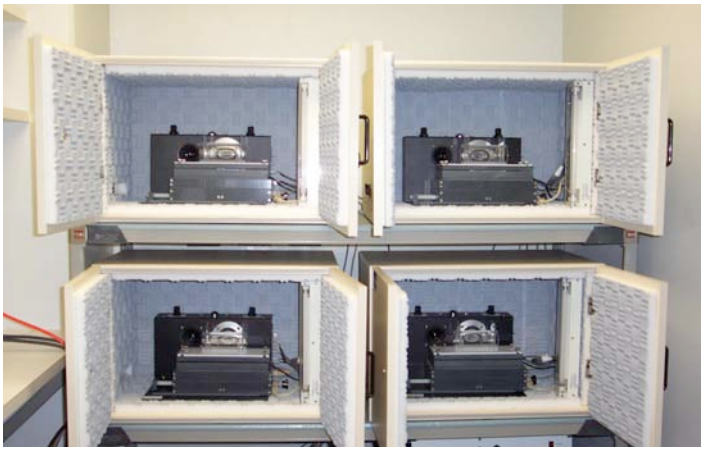

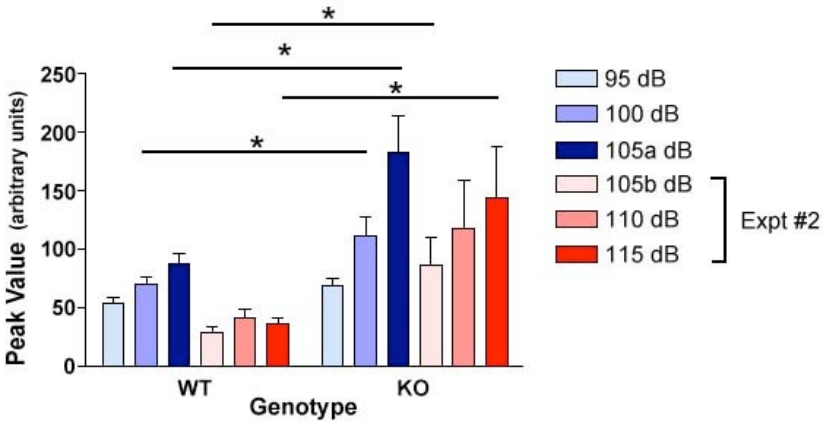

All animals were tested for basal startle responses, as described in Current Protocols in Neuroscience (2003). Four startle boxes (Med Associates, St. Albans, VT) were used (shown above). Background white noise (65 dB) was present at all times. After a 5 min acclimation period, 45 white noise pulses (95, 100, and 105 dB, 15 for each intensity) were presented on a randomized schedule with average 30-sec variable intervals. Two weeks later, the test was repeated. As shown in the graph above, both WT and KO mice showed increasing startle amplitudes across the dB range, and KO mice had greater amplitudes than WT mice at the 105 dB level ($p < 0.01$).

Fear Conditioning

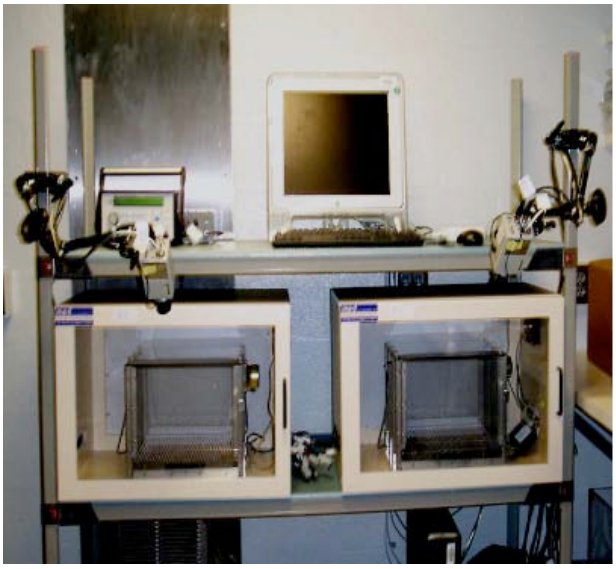

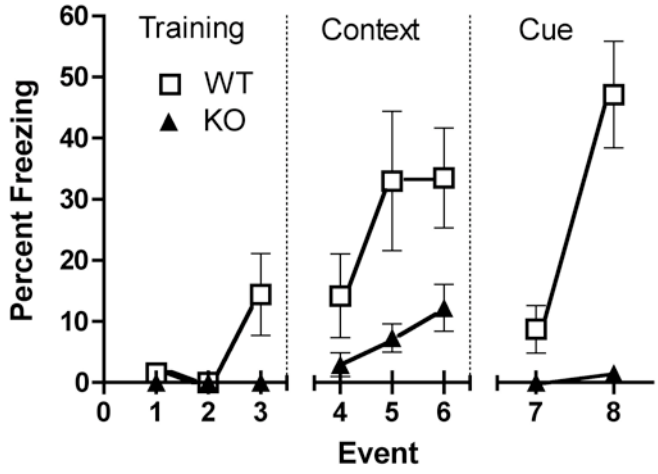

Fear Conditioning was conducted the following week. Fear conditioning was done in two fear conditioning boxes, shown at left (Med Associates, St. Albans, VT) using Actimetrics tracking software (Evanston, IL) as described elsewhere (3). During cued test session a modified chamber with different floor and walls was used. Different smells and lighting are used as well.

The training session was done on day one, and on the following two days, mice were tested first for contextual and then cued fear conditioning. Animal movements were recorded by video camera and freezing was quantified by Actimetrix software as percent of time when animals remained immobile.

Training: animals were placed in the chamber, and after 2 min they were presented with a 30-sec 2800 Hz 40 dB tone co-terminating with a 2-sec 0.7 mA shock followed by a 30-sec post-shock period. Both WT and KO mice showed considerable jumping and running during the period of shock presentation, and there were no differences in their activity during shock delivery (611 ± 64 for WT; 562 ± 28 for KO mice; numbers are activity in arbitrary units representing cumulative locomotion during the shock period ± SEM). The WT mice showed some freezing during the tone presentation and even more freezing after the shock, and significantly more freezing than the KO mice at these later times. In fact, the KO mice showed absolutely no freezing throughout the training session (before shock (0 ± 0), during tone (0 ± 0), or after shock (0 ± 0)).

The following day, in the context condition, both KO and WT showed more freezing behavior than they had during the training session, increasing in amount during the course of the test session. For both KO and WT groups, significantly more mice froze in the second and third minute of the context test than they had in the first minute of the training session ($P < 0.001$ for KO and $p < 0.02$ for WT, Chi Square test). The percent time spent freezing increased for both groups, but the increase was not significant for KO mice ($p = 0.07$), analyzed either by total time or individual min. Comparing groups, WT percent freezing was significantly higher than KO in the last 2 min of the 3-min session.

On the third day, in the 3-min cued test, with all context information removed, freezing was measured before and during tone (cue) onset. The tone was the same as that presented in the training session. It was given as a single tone beginning after 1 min and continuing for 2 min until the end of the session. Both KO and WT mice showed significantly more freezing after the cue than before the cue (F test, main effect cue, $p < 0.001$; post hoc tests were paired T tests: WT significant at $p = 0.01$; KO significant at $p < 0.05$). However, when comparing groups in each of the conditions, significant differences between genotypes only appeared in the pre-cue condition, in which the WT mice froze significantly more than the KO mice. Thus, the cue elevated freezing behavior in both groups, and though cued freezing behavior was about 3-fold higher in WT compared to KO, the difference was not significant ($P = 0.07$).

The data (figure above) show that compared to WT mice, the p50 KO mice have a greater startle amplitude at 105 dB, suggesting a hyperreactivity to stimuli, but they do not freeze in novel situations or immediately in response to electric shock. The p50 KO mice show context-dependent freezing and thus display both fear and fear memory, but context-dependent freezing is not as great as for the WT mice. KO mice also show cued-based memory of the shock and are not significantly different from WT in the amount of freezing shown. The startle and fear conditioning data together suggest that the p50 KO mice are sensitive and reactive to stimuli, but they do not adapt to repeated aversive stimuli and fail to show a "normal" response to their context (i.e., by freezing). They register the aversive event, and they remember it, but its emotional valence is greatly reduced. They also show reduced fear- or anxiety-like responses to novel environments and are not prone to freeze.

Resident–Intruder task

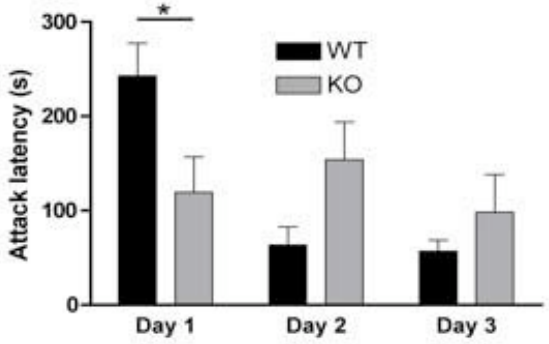

A stranger mouse, having been raised in a group-housing condition, is placed into the home cage of the resident mouse. Interactions between the resident and intruder are recorded over the course of the next 15 min, after which the intruder is removed. Mice were assigned random numbers so that scorer was blind to genotype. All testing occurred during the dark cycle. Mice were given 2 min after initial aggressive encounter, with a maximum of 5 min before session was terminated. If no attack occurred within 5 min, attack latency was considered to be 5 min. An aggressive encounter was defined as biting, attacks, lunging, and rolling around. Mice were tested once a week for 3 consecutive weeks.

Immobilization stress and the HPA axis response

We had found that the p50 KO mouse appeared to be relatively more stressed in a 2-h immobilization experiment relative to WT, based on recordings of body temperature during the stress period. This kind of stress produces rapid hypothermia that continues for the duration of the stressor. The drop in temperature is greater in KO than WT mice (see 2003 BSC report). We decided to fully characterize the stress axis in these mice, following the protocols developed in our lab previously for using ISHH to show changes in gene expression levels in key areas responsible for setting levels of activity in the hypothalamic-pituitary-adrenal (HPA) axis (4).

The results of an exhaustive ISHH study in which immobilization stress for 1, 2, or 6 h was followed by analysis of mRNA expression of a battery of genes (CRH, POMC, TH, GAD65 and 67, 5-HT1A, GR, MR, and c-fos) expressed in stress-circuit brain regions (PVN, BNST, Hippocampus, LC, and pituitary) showed no differences between WT and p50 KO mice (table below).

Expression of mRNAs in NFkB1-/- (p50 KO) mice and WT controls after single 2 h immobilization

	WT		p50 KO	
Region/ probe	no stress	stress	no stress	stress
GR				
CA1	2751 ± 407.5	2077 ± 166.0	3970 ± 426	1871 ± 179[1,2]
CA3	1063 ± 119.9	762 ± 65.2	1624 ± 242	797 ± 65[1,2]
DG	2209 ± 213.3	1516 ± 98.0	6317 ± 414	1515 ± 144.[1,2]
MR				
CA1	2834 ± 186	2541.0 ± 123.7	2283.4 ± 221.9	2604.9 ± 159.7
CA3	1671 ± 61	1476.3 ± 81.4	1422.9 ± 114.7	1513.7 ± 103.7
DG	2503 ± 131	2103.0 ± 78.4	2150.9 ± 238.8	2369.5 ± 174.8
TH				
LC	8623 ± 595	12605 ± 1056[3]	10268 ± 850	13380 ± 605[2]
Gad 65				
BSTM	1556 ± 169	1968 ± 236	1735 ± 311	1872 ± 82
BSTLV	1322 ± 59	1339 ± 139	1238 ± 196	1292 ± 44
peri-PVN	1994 ± 110	3254 ± 964	2383 ± 547	2067 ± 88
Gad 67				
BSTM	885 ± 176	659.6 ± 49	1253 ± 238	748 ± 39
BSTLV	1081 ± 212	807.6 ± 49	1375 ± 256	852 ± 24
peri-PVN	1307 ± 70	1318.3 ± 146	1136 ± 68	1088 ± 98
CRH				
PVN	163.0 ± 24.6	476.0 ± 46.2[3]	174.7 ± 23.0	444.4 ± 54.2[2]
mTPH2				
DRI rostral	25232 ± 2257	29267 ± 2186	22986.1 ± 2001	22038 ± 1569
DRI caudal	16613 ± 2353	13083 ± 1316	13519.3 ± 1055	10766 ± 1735
DRD/DRL	25008 ± 1598	30799 ± 1750	30706.8 ± 1638	30720 ± 1193[1]
MR	18941 ± 1670	22335 ± 1622	20317.6 ± 1139	21738 ± 1141
5Ht1A				
CA1	1290.5 ± 84.1	1471.3 ± 118.1	1382.0 ± 101.1	1540.0 ± 67.7
CA3	425.8 ± 20.5	453.4 ± 16.2	467.7 ± 19.3	486.1 ± 63.1
DG	501.3 ± 57.8	483.3 ± 25.5	508.7 ± 29.2	485.2 ± 60.6

c-fos				
*IL	37.2 ± 4.3	66.6 ± 7.1[3]	48.9 ± 5.0	64.8 ± 6.7
*PrL	25.6 ± 2.6	87.4 ± 16.9[3]	43.1 ± 6.7	77.3 ± 9.4[2]
BSTM	53.1 ± 19.9	92.0 ± 12.0	69.1 ± 23.9	78.6 ± 18.6
BSTLV	54.7 ± 16.3	73.4 ± 12.9	71.9 ± 19.6	106.4 ± 26.2
PVN	72.0 ± 29.6	414.0 ± 36.6[3]	47.9 ± 14.3	481.3 ± 15.4[2]
LC	85.4 ± 15.0	328.6 ± 34.7[3]	68.3 ± 8.9	462.3 ± 50.0[2,4]
AP	73.3 ± 12.2	106.2 ± 10.1	75.2 ± 10.1	170.0 ± 16.5[2,4]
NTS	72.5 ± 8.7	107.9 ± 8.6[3]	94.7 ± 5.0	127.1 ± 10.6[2]
POMC				
ant lobe	348.5 ± 50.8	584.4 ± 140.6	473.3 ± 69.7	405.9 ± 53.0
inter lobe	23639 ± 6369	31997 ± 3421	31782 ± 5463	24392 ± 3417
CORT	47.5 ± 10.5	502.5 ± 56.1[3]	29.2 ± 6.3	567.3 ± 28.3[2]

[1] significant difference in no stress condition b/t WT and p50 KO ($p < .05$)
[2] significant difference in stress vs. no stress in p50 KO ($p < .05$)
[3] significant difference in stress vs. no stress in WT ($p < .05$)
[4] significant difference in stress condition b/t WT and p50 KO ($p < .05$)
Values represent the mean optical density ± SEM
* Values represent mean optical density X area ± SEM

Summary

- Both WT and KO mice showed increasing startle amplitudes across dB range, however KO mice had significantly greater startle amplitudes at 100,105a, 105b, and 115 dB.
- Both WT and KO mice appeared to have both context and cued-based memory of the shock treatment.
- KO mice froze significantly less than WT mice during the second and third minute of the context situation and before and after cue presentation.
- KO had significantly shorter attack latencies in comparison to WT mice only on day 1 of the resident-intruder test.
- The HPA axis in the p50 KO mouse appears to function normally in response to stress

Behavior—C57BL/6 NFkB1-/- mouse

The following experiments were performed in 2006 by Michael Lehmann after we obtained the NFkB1-/- on the pure C57BL/6 background.

Elevated Plus maze:

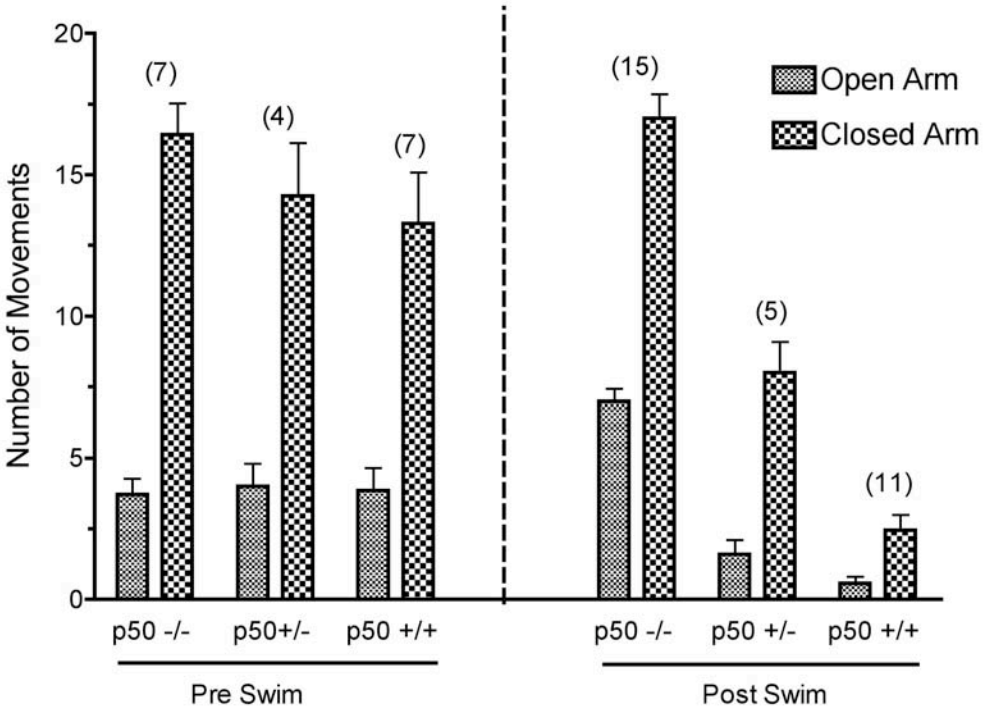

Number of movements in Elevated Plus Maze with no prior stressor (pre-swim) or 10 min after a 15 min forced swim (post-swim). Number in parenthesis denotes animals in group

Basal anxiety levels can be interpreted by the amount of time/ number of explorations the animal spends on the open arm of the elevated plus maze (EPM). There were no differences between KO and wildtype open arm explorations (Figure above, left side), suggesting no differences in basal anxiety levels. A second experiment was designed to increase anxiety before placing animals on the EPM. KO and WT mice were subjected to a 15 min forced swim, allowed a 5 min rest and then placed on the EPM for 10 min (Figure above, right). A 15-min pre-swim had no effect on the p50 KO group activity compared to the non-swim group. However, the forced swim significantly curtailed both open and closed arm activity in the WT animals. The non-effect of swim stress on KO performance suggests that stressors do not have adverse effects on the emotional state of the p50 KO animal.

Morris Water Maze:

The Morris Water Maze (MWM) was used to reveal changes in hippocampal functioning between p50 KO and WT animals. The MWM consists of a circular pool 150 cm in diameter filled with water made opaque with white crayola latex paint. A small clear Plexiglas escape platform is placed 1 cm under the water surface. The acquisition phase consisted of five consecutive training days with four trials per day. On each trial mice were placed in one of four starting locations facing the pool wall and allowed to swim until finding the platform, or until a maximum of 60 sec. Subjects are considered to have spatially learned the maze if they can find the location of a hidden platform in under 15 seconds. Shown in the Fig. above, the p50 KO mice showed significant improvement in time to hidden platform, learning the location of the hidden platform by day 3 compared to day 5 for the WT mice. The MWM could be considered a stress inducing experiment; therefore performance reflects spatial memory formation under duress. The increased spatial learning performance in the p50 KO mouse relative to WT mouse could be due to stress-induced enhanced performance.

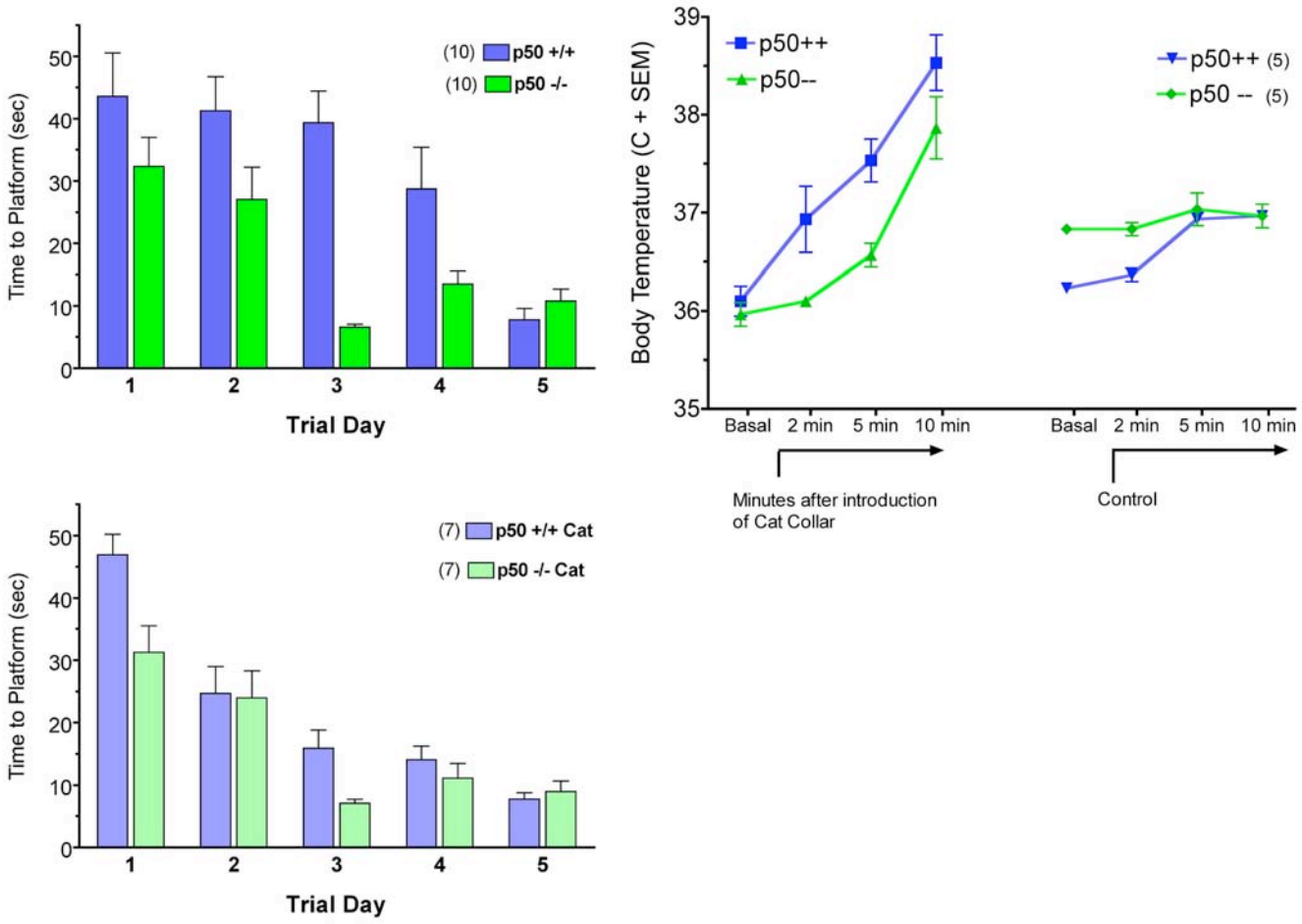

In a second experiment, animals received a 10 min exposure to a used cat collar before the start of the first trial on each of the five days. Research has shown that predator odor exposure is one of the strongest psychological stressors. Temperature transponders (BMDS) implanted subcutaneously in the mice indicated that exposure to the worn cat collar had a pronounced effect on the hyperthermic stress response compared to exposure to an unused cat

collar (Figure, above right), and much more so in the WT than p50 KO mice. A two-way ANOVA reveled a significant interaction between odor exposure and time to platform. WT animals exposed to predator odor showed a significant improvement in the MWM compared to controls (Figure above). No significant improvement was recorded in the p50 KO mice. The results suggest that acute increase in anxiety confers a benefit towards solving the MWM, which is seen in the WT mice but not the KO mice because of a ceiling effect in the latter.

Barnes Maze:

The Barnes maze is similar to the MWM in that it tests spatial learning ability but without the inherent hi-stress swim component. For this test, a 100 cm maze with 21 possible exits was set up in a low light arena, with minimum noise and no air current. One of the holes has a burrow, made of opaque Plexiglas. Animals were placed under an opaque dome in the middle of the Barnes maze and allowed to acclimate to the surface for 1 min. Once the dome is lifted the animal is able to orient to distant spatial cues and find the hole with a hidden burrow. Acquisition phase consisted of four consecutive training days with four trials per day. Each trial lasted five min. The maze was rotated and the surface cleaned with 70% EtOH between trials to remove any odor trails, although the burrow was kept in the same spatial position. A one-way ANOVA of the 'time to finding burrow' (Prime TIme) revealed a significant main effect of trial day; post hoc analysis revealed that both WT and p50 KO mice showed significant improvement towards finding the goal on day 2 (Figure below). No difference was observed between genotype groups, suggesting that the improved performance in the MWM was related to anxiety associated with the MWM.

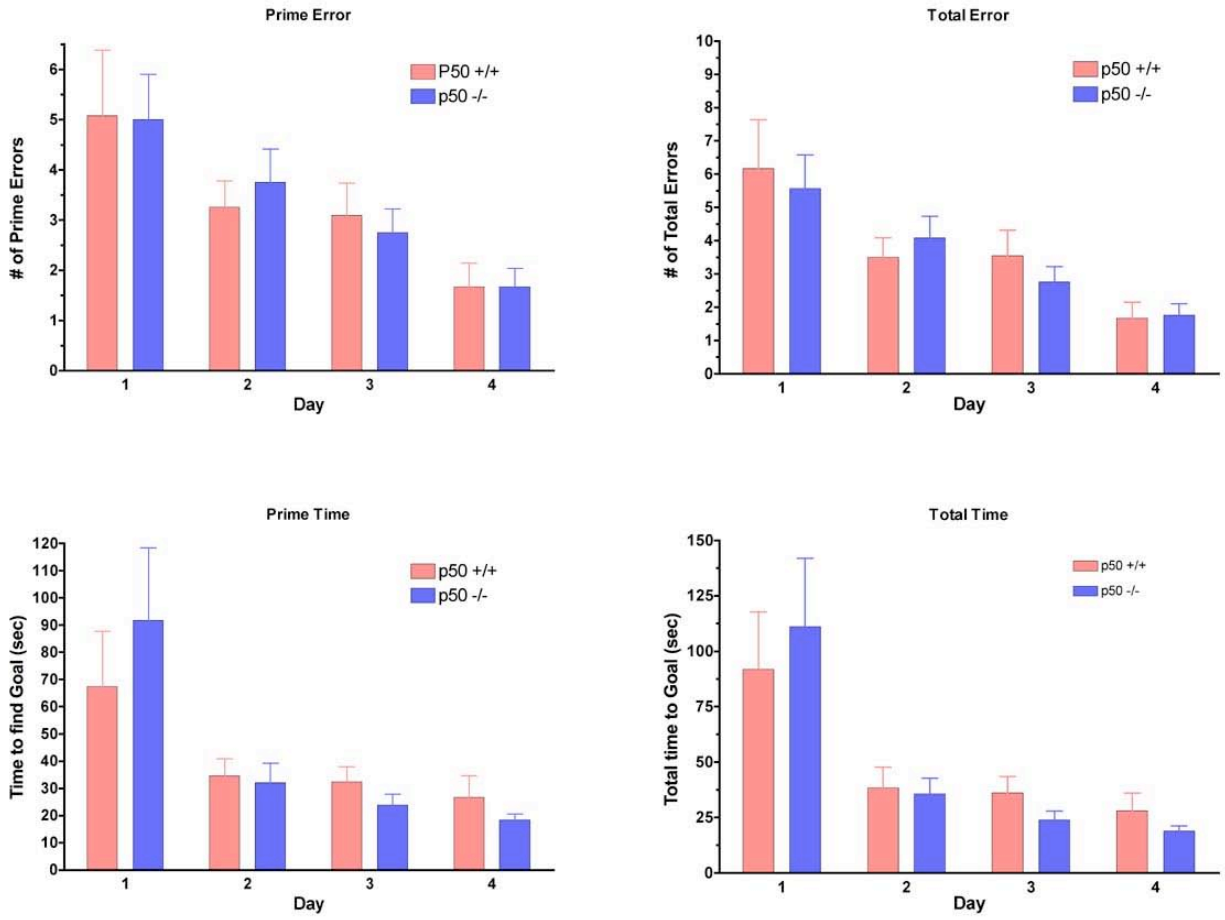

Physiological Measures:

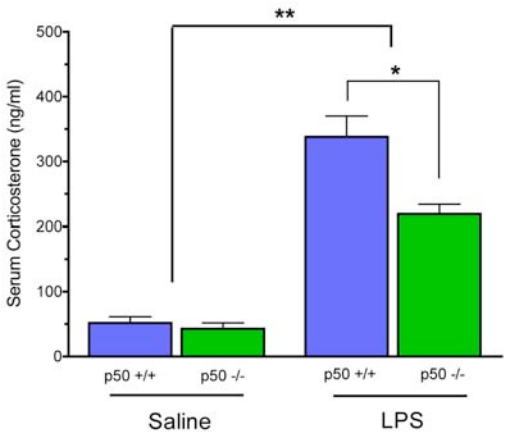

Corticosterone (CORT) was measured from trunk blood of p50 KO and WT animals 60 min after injection 0.4 ml Saline Vehicle, or 0.1mg/kg LPS (Figure at left). Trunk blood was also sampled during the 5:00 PM circadian surge period. ANOVA revealed a significant effect of treatment, post hoc analysis revealed a significant increase in CORT response to LPS in WT compared to p50 KO animals. The data support the conclusion that the p50 KO mouse does not respond as robustly to stressors as does the +/+ littermate counterpart.

Hot Plate Analgesia:

This test measures the latency of a mouse to lick its paw, jump, or shake in response to heat exposure. Hot plate is set to 55°C. Values are recorded in seconds. ANOVA found no significant difference between genotypes, or sexes (not shown). The data indicate that diminished responsiveness to aversive stimuli in p50 KO mice is not due to a sensory defect.

Fear conditioning:

Animals were placed into the training chamber and allowed to explore for 2 min, after which they received an electric shock (1 sec, 0.5 mA). The 2 min/1 sec shock paradigm was repeated for a total of three shocks. After the last shock, animals were allowed to explore the context for an additional 1 min prior to removal from the training chamber. Freezing behavior was measured at either 24 h or 7 days after fear conditioning by placing the animals back into the chamber. Freezing behavior was measured for 4 min. There were no significant differences between groups, indicating that fear memories are intact in the p50 KO mouse, and unlike its counterpart on the 129/BL6 background, the C57BL6 p50 KO mouse is fully able to show freezing behavior in a cued context.

Summary:

The phenotype of the p50 KO is dependent on the strain background, which has been reported for a number of knockouts, often with much more dramatic consequences. There are some data that suggest similarity of behaviors between KO mice on the 129/BL6 background versus the pure BL6 background, however. In both conditions, anxiety behavior is altered. On the 129/BL6 background, the resistance to anxiety was more up-front and immediately apparent, whereas on the pure BL6 background, prior exposure to stressor was required to make it evident. In performing these studies, we uncovered an important emotional component to spatial learning assessed in the MWM, which is an aversive task especially to mice. The data from the BM and the fear conditioning experiment indicate that the p50 KO mouse does not have impairment in learning or memory. Recently the p50 KO mouse on the 129/BL6 background was subjected to the MWM and shown to have no difference in learning compared to its non-genetically matched WT counterpart (for example, KO mice and “matched” WT mice from JAX have completely different coat colors). The difference in outcomes in the same task

in that study and ours underscores the need to take emotional factors into account when attributing a learning/memory cause to an acquisition score.

Maternal Immune Activation (MIA) Research Design and Methods

Procedure: Maternal Immune Activation in rats:

Dams (Sprague-Dawley) will receive a 0.5 mg/kg i.p. injection of the bacterial endotoxin LPS (Sigma, serotype 055:B5) on gestational day 15. To verify the presence of a maternal immune response, some dams will be sacrificed 4 h post LPS injection and trunk blood and the spleen will be collected and analyzed using rat specific ELISA assays.

Behavioral Assessments:

1. *Juvenile Play*

Postnatal day 18 offspring will be paired with a novel stimulus rat matched for sex and size, and placed in a clean, empty rat holding cage and videotaped for a 10-minute interaction period. Social parameters include number of nose-nose sniffing and social grooming bouts, and number of pushes and crawls made by the testing rat.

2. *Elevated Plus Maze*

Anxiety will be assessed in post-natal day (PND) 24 offspring using a standard rat elevated plus maze. Trials will be recorded and scored for number of entries and time spent in the open and closed arms.

3. *Social Preference*

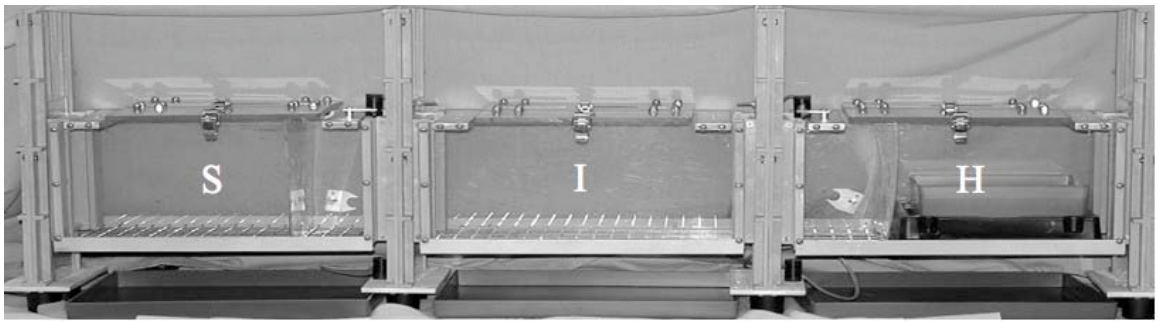

A three-chambered automated social task will be used to measure the preference to investigate a novel stimulus rat versus investigation of a non-social, familiar home environment in rats across development (PND 25, 33, 45, 55). The experimental apparatus consists of home chamber that contains bedding from he home cage, a social chamber that contains a stimulus rat, and an initial chamber where the test subject is placed. Number of entries and time spent in the home and social chambers are recorded.

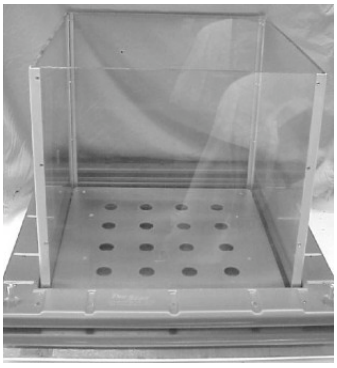

4. *Exploratory Behavior*

An automated hole-board task will be utilized to record frequency of exploration in rats across development (PND 25, 33, 45, 55). The floor of the apparatus consists of a 16-hole matrix hole-board platform with each of these holes cupped at the bottom, where a few kernels of fresh bedding are placed. Computer software records exploration, defined as the number of

nose-hole entries each rat conducted per minute of ambulation around the chamber. Additional locomotor information, including total distance traveled, total number of movements, and the path traveled, is recorded.

Minocycline Treatment

If neonates (PND 10) born to LPS-moms show enhanced microglial activation as shown by qRT-PCR, a treatment group will be added to the experiment. Mothers and offspring will receive minocycline (45 mg/kg, i.p.) or vehicle (PBS) twice: to the mother immediately after LPS injection and to the offspring at PND 2.

Primary hippocampal and neocortical neuronal cell culture

History of optimization

In 2005 Priyanka Rathore began a concerted effort to establish the role of NF-κB in neurons in vitro. Neurons, but not glia, had been reported to have NF-κB activity after stimulation by glutamate (5-8). We therefore focused our efforts on glutamate as a stimulus. Data showing that glutamate activates NF-κB in neurons comes mainly from cultures on primary cerebellar granule cells. These neurons appear unique in numerous ways, and work done on NF-κB activation in cerebellum *in vivo* is inconsistent, implicating NF-κB activation in young but not adult animals. In neocortical or hippocampal neurons, activating NF-κB is much more difficult. The Kaltschmidts had done extensive work in primary neuronal cell culture, and so did Barger's group. Given Barger's point that even small amounts of glial contamination could create a strong NF-κB signal of glial origin in a neuronal culture, we tried to reduce or eliminate glia in the cultures. The growing conditions were optimized over many experiments with modifications in growing medium and growth duration. Embryonic day 16–18 mouse embryos were dissected with careful removal of meninges and isolation of neocortex and hippocampus. Growth was in Neurobasal medium (+B27 supplement, Gln, and Glu), similar to other published work. Attempts to kill glia using C-arabinoside caused neuronal damage at any concentration, so they were abandoned. Immunostaining of cultures with GFAP and NeuN antibodies indicated that <10% of the cells were astrocytes, and the remaining cells were neurons. Western blots with GFAP antibodies showed no bands in the neuronal cultures (Appendix).

Co-culture

The notion of using co-cultures was initially very attractive. Given the findings that neuronal growth and establishment of proper synaptic connections is greatly facilitated by the presence of glia, we wanted to have glia in the culture. However, as mentioned before, any assay must be done on just the neurons in the absence of glia. Furthermore, given our plans to use pure neuron preparations for assays like microarray and quantitative PCR, a method for separating the neurons from glia at the end of the assay was needed. Thus, neurons were grown on coverslips sitting on tiny paraffin dots above the tissue culture wells coated at the bottom with a glial bed grown separately. For assay, the coverslips were either left in place or they were removed to another well to permit examination of responses without the contribution of the glia and the glia-conditioned medium.

We performed glutamate toxicity studies with the co-cultures, assaying cell death by Nissl staining, the MTT method, or using the LIVE/DEAD assay. Nissl staining showed cells with dark nuclei at 10–20 μM glutamate, and at higher doses (> 100 μM), the cells looked disrupted. This low-dose toxicity, confirmed by the other assays, occurred in the presence or absence of

the glial layer, contrary to some other findings in the literature. Also, the neurons grown in presence of glial layer showed higher constitutive activity as compared to neurons grown without glial layer. Furthermore, in looking at immunohistochemical results after drugs were given to sandwiched assemblies, it was apparent that slow drug diffusion between the layers was a significant confound. We decided to abandon the co-culture approach.

Final culture conditions.

Mouse hippocampal neurons were cultured from 16-day embryonic mice as described previously (9). Hippocampi or cortices were dissected out in cold Hanks balanced salt solution (HBSS) after careful removal of meninges and trypsinized (final 0.05%) for 15 min at 37°C. Following digestion, the hippocampi or cortices were washed twice with Dulbecco's modified Eagle's medium (DMEM) containing 10% fetal bovine serum (FBS) and triturated. The cells were purified using a 40 μm nylon strainer and seeded onto poly d-lysine coated coverslips at a density of 0.12 x106 cells/well for immunocytochemistry and in 6-well plates at 2 x 106 cells/well for Western blots, and maintained at 37°C in the presence of 5% CO2/95% O2. After 24 h, DMEM was replaced with Neurobasal medium (Invitrogen) containing B27 supplement (Invitrogen) and 2 mM Glutamax I (Invitrogen). After 7 days in culture, cells were processed for immunostaining and immunoblotting.

Selection of phosphorylation of p65 at serine 276 as the neuronal readout.

Concurrent with these efforts, we applied a number of antibodies to the cultures in attempts to show glutamate-induced nuclear translocation of NF-κB subunits. Most of the antibodies used for Western blots were also used for immunohistochemistry of cells in culture (see list). The antibodies, using standard staining protocols and a variety of antibody dilutions (typically 1:500), showed extensive cytoplasmic and nuclear staining that was not altered in any way by any of the glutamate treatments. Only one antibody showed a selective and dramatic

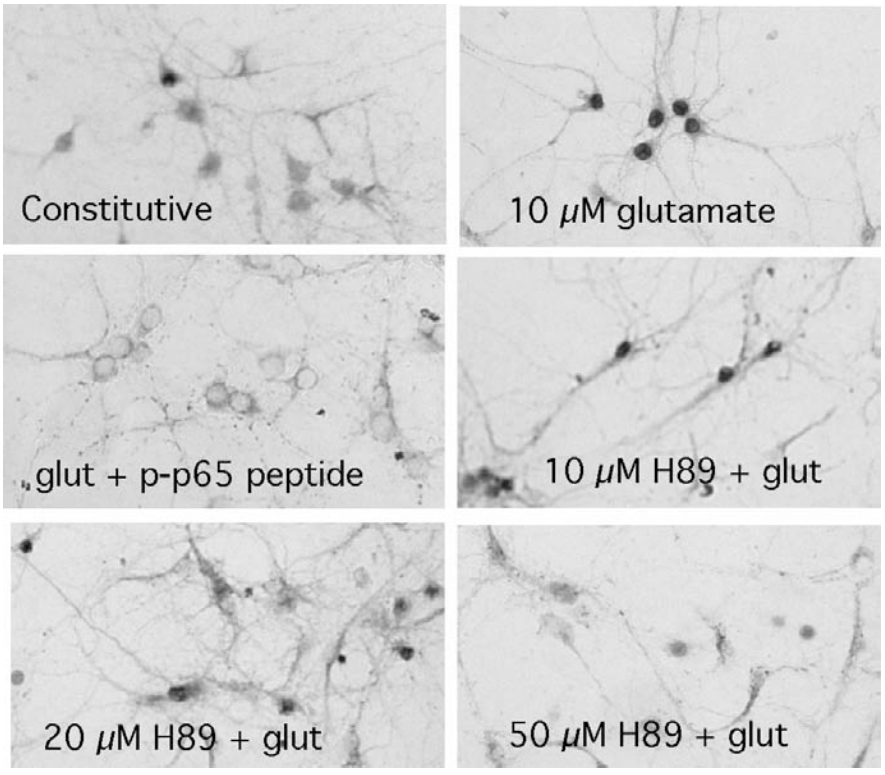

The phospho ser276-p65 staining appears in the nucleus of hippocampal neurons 10 min after 10-μM glutamate. The immunostaining is blocked by the peptide the antibody was raised against. H89 dose-dependently inhibits the nuclear staining.

response that appeared appropriate to its function. The rabbit polyclonal to NF-κB p65 phosphorylated at ser276 (#3037; Cell Signaling) showed dramatic appearance of nuclear staining following glutamate treatment (Figure above). The nuclear staining was selectively eliminated by co-incubation of the cells in the presence of excess phospho-p65 peptide. Finally, the nuclear staining was blocked dose-dependently by the PKA and MSK-1 blocker H89. Linda Vermeulen had shown that p65 was phosphorylated at ser276 by MSK-1 in fibroblast cells following TNF stimulation (10).

Quantification of results shown in previous figure.

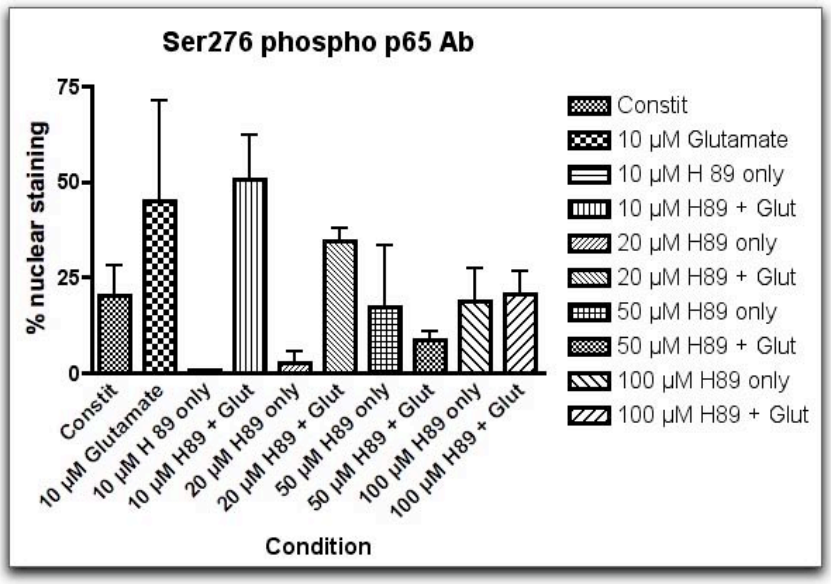

Phosphorylation and acetylation of the p65 subunit are two posttranslational modifications required to generate a fully active NF-κB complex (11-14). Phosphorylation of p65 at various serine residues (276, 529, and 536) enhances its transactivating potential (15). Several kinases have been postulated to phosphorylate p65 including Casein kinase II, Akt, IKK, protein kinase A (PKA), and p38 mitogen- and stress-activated protein kinase-1 (MSK-1) (10, 15). The mechanisms by which p65 phosphorylation enhances NF-κB transcriptional activity may involve the recruitment of various transcriptional co-activators (CBP/p300) at promoter sites (16).

The results emboldened us to look for upstream and downstream signaling pathways in neurons that lead from glutamate stimulation to p65 translocation and activation. Toward that end, a Western blot analysis was conducted.

In the highly enriched neuronal cultures, immunocytochemistry and Western blot analysis showed the presence of constitutive staining with the phospho-ser276-p65 antibody, suggesting IκB-independent actions of NF-κB subunits (15). This NF-κB constitutive activity was significantly depleted upon removal of extracellular calcium ions by the addition of EGTA (1 mM) to the medium. Glutamate (10 μM for 10 min) treatment in these EGTA-pretreated neurons increased the concentration of phospho-ser276-p65 in the nuclei as detected by Western blot analysis of nuclear and cytosolic extracts. Similar effects of EGTA and 10-mM glutamate were observed for CREB phosphorylation using a phospho-CREB antibody. Phosphorylation at serine 536 of p65 subunit was also tested in the glutamate-treated hippocampal neurons, but no signal was detected, indicating that this phosphorylation site may

not be involved in NF-κB activation pathway in neurons or astrocytes. HeLa cells were very responsive to TNFα (see below).

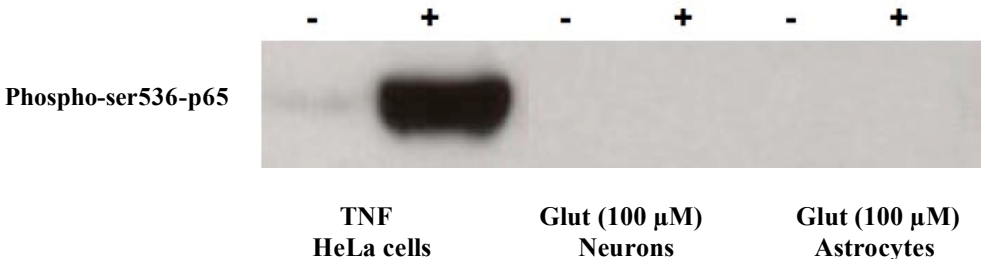

To assess what signaling pathway mediated the glutamate induced phosphorylation of CREB and p65 subunit, western blot analysis of hippocampal neurons treated with inhibitor of PKA (H89), MAPK (U0126, PD98059), p38MAPK (SB203580) was performed. Complete blockade of NF-κB constitutive and 10 μM glutamate induced activity was observed with treatment of 30 μM of H89 (PKA inhibitor).

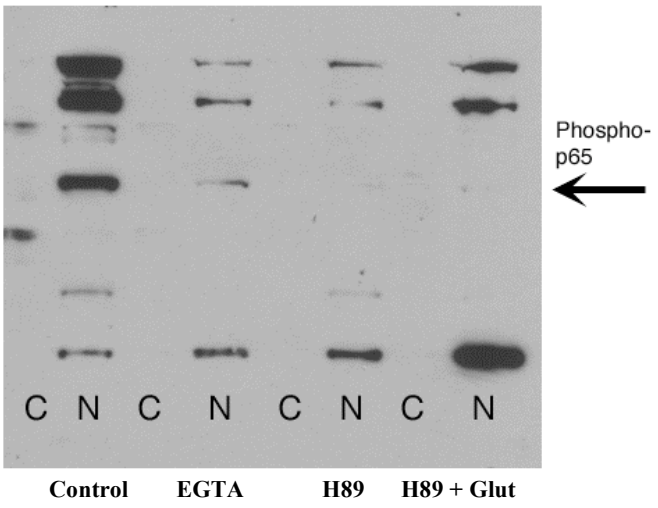

The other kinase inhibitors used (alone or in combination) did not block either the NF-κB constitutive activity or the glutamate induced phosphorylation of p65 subunit. Interestingly, p-ERK1/2 was significantly upregulated in glutamate-treated hippocampal neurons.

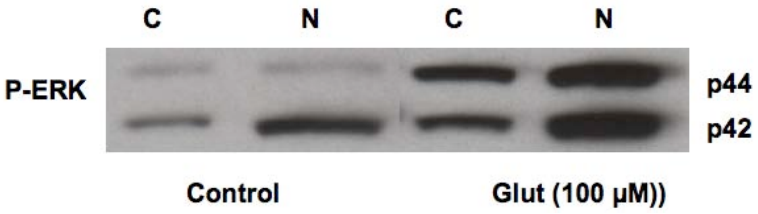

Since the initial step of phosphorylation was observed in the glutamate-stimulated neurons, occurrence of DNA binding and transactivation was tested. EMSA analysis showed a

glutamate dose-dependent (10–500 μM) increase in DNA binding activity of NF-κB. The effect of H-89 on glutamate induced DNA binding was also tested. H-89 completely blocked the glutamate induced NF-κB DNA binding. Further, supershift assay using p65 and p50 antibodies was conducted to detect the composition of the dimer. The assay indicated that the binding partners are p50 and p65. The p50 antibody completely shifted the dimer while p65 antibody always diminished the band intensity and no shifted band was seen

Very little or no GFP fluorescence depicting transcriptional activation of the NF-κB reporter system was detected in transfected hippocampal neurons.

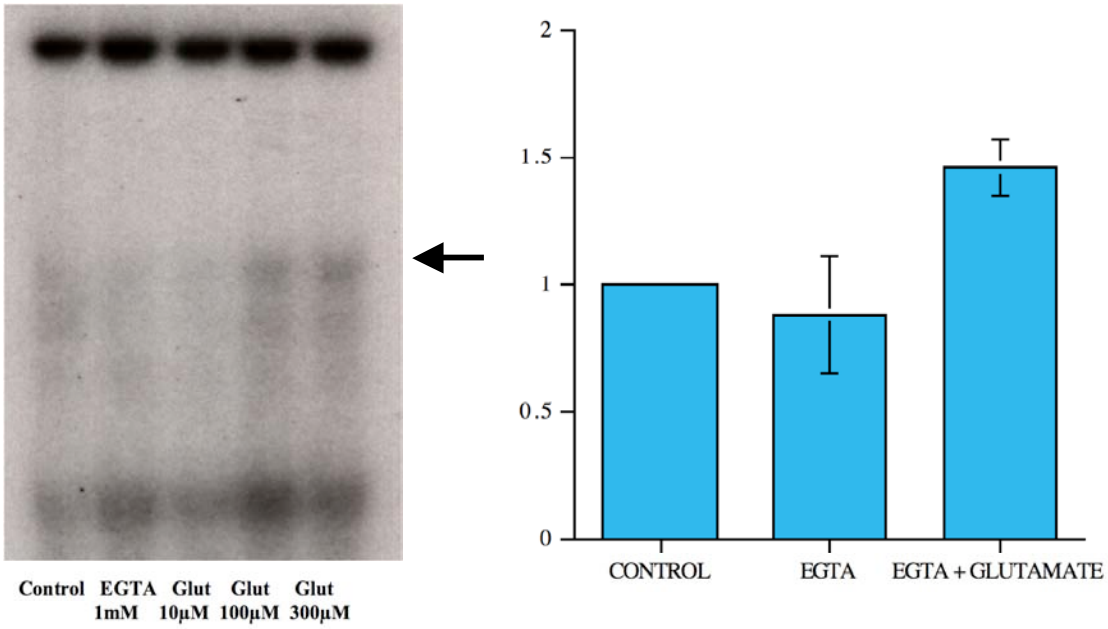

T

The graph is representative of significant DNA binding induced by 100 μM dose of glutamate. N=3 separate EMSA experiments were conducted in nuclear extracts obtained from hippocampal neurons stimulated with 100 μM glutamate. Result was expressed as Mean $\pm$ SD.

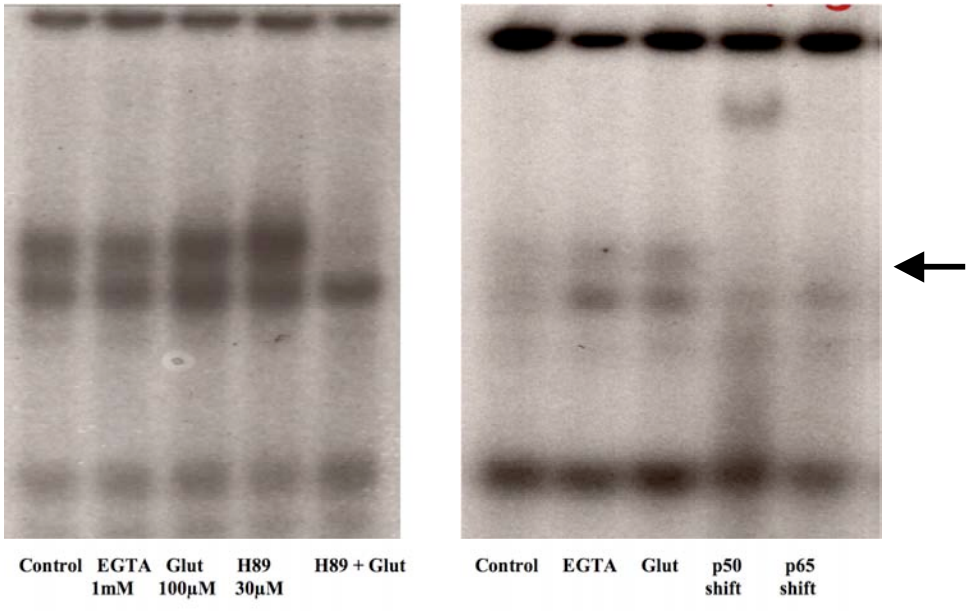

Conclusion

The study indicates that restricting calcium fluxes and blocking kinases that phosphorylate p65 control the constitutive nuclear p65 phosphorylation state. Phosphorylation of p65 at serine 276 may be part of the cell's response to glutamate, leading to a small increase in κB DNA binding activity in neurons. Regulation of p65 phosphorylation in neurons might involve multiple Ca^{2+} dependent/independent and PKA/MSK-1 pathways.

HIV LTR-lacZ κB reporter mouse

As stated, our goal has been to develop neuroanatomical tools that will afford evidence of NF-κB activity at the single cell level in order to better assess the specific role of neuronal NF-κB activity. Using antibodies to track nuclear translocation of NF-κB subunits is one approach, and thus far the tools have not been satisfactory. Another way to track NF-κB is to use tools that provide cellular resolution of NF-κB/DNA binding to kB sites. The canonical DNA sequence that NF-κB dimers bind to after translocation to the nucleus is GGGACTTTCC, and the consensus sequence is GGRNNYYCC. There are several ways to visualize the binding of NF-κB dimers to this sequence. One method to do this is Southwestern hybridization histochemistry, in which a labeled double-stranded oligonucleotide probe is applied to tissue where it binds the nuclear dimers. This has been reported to work for NF-κB (17). However, two fellows attempted and failed to make this technique work in our lab.

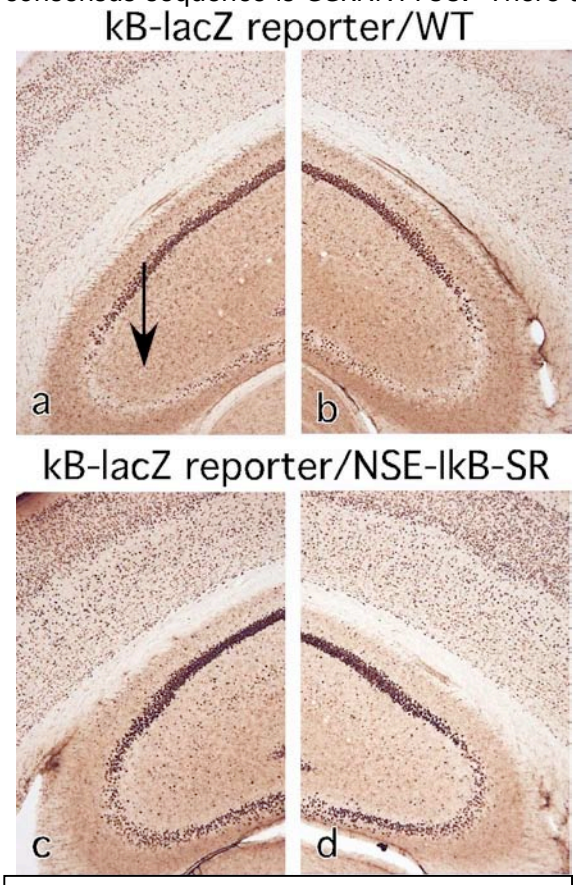

Fig 6. Intrahippocampal kainate injection (arrow) did not alter kB expression levels 15 min after injection into CA3 (a vs. b). In addition, presence of neuron-specific inhibition of NF-kB slightly increased, rather than decreased, levels of constitutive kB reporting (a,b vs. c,d).

Another way is to use a transgenic mouse containing a κB reporter construct. A striking finding with one of these animals was constitutive kB reporting (revealed by beta-galactosidase staining) in neurons of embryonic and adult mice (18). We acquired this HIV LTR kB-lacZ reporter mouse, which contains multiple copies of the canonical κB site upstream of lacZ, and confirmed the constitutive neuronal expression by staining with beta-galactosidase and by beta-gal immunohistochemistry. In order to determine whether this level of expression can be modified by manipulations involving neuronal NF-κB activation, we crossed this mouse with another transgenic mouse we acquired that has neuron-specific suppression of NF-κB activity. The NSE-IkB-super repressor (NSE-IκB-SR) mouse has a transgene that expresses a serine-mutated IkB that is unable to be phosphorylated and thus cannot be degraded (19). In a single experiment, kainate was injected into the CA3 field in three kB-lacZ reporter mice and also in three reporter mice that had been crossed with transgenic mice containing the NSE-IkB-SR construct that

selectively inhibits neuronal NF-κB activity. We had two expectations from this experiment. First, the levels of kB reporting might rapidly respond to the excitatory stimulus (for example, Romano's group have recently reported that κB reporting, measured by EMSA in the hippocampus, changes at 15 min following exposure of mice to an inhibitory avoidance paradigm (20, 21). Second, universal neuronal NF-κB inhibition by the IkB super repressor construct, would diminish neuronal κB reporting in the double transgenic mice, similar to what was reported in transgenic mice containing a kB reporter plus tetracycline-conditional inhibition of neuronal NF-κB activity (22). However, neither expectation was realized: the kainate stimulus was without effect on lacZ reporting, and the existence of the NSE-IκB-SR construct did not diminish lacZ reporting in neurons. In fact, the opposite occurred. As Fig. 6 shows, the mice with the IκB-SR construct actually had higher levels of β-Gal immunostaining in hippocampal and cortical neurons. One possible explanation for the paradoxical effect is that removal of NF-κB dimers from the nucleus permitted Sp1 transcription factor binding to the kB site, as has been shown in other models (23). The findings dramatically reduced our enthusiasm for using the κB-lacZ reporter mouse and called into question the usefulness of the NSE-IκB-SR mouse. I

Generation of a mouse-specific p50 antibody

Pierre Brown used his immunohistochemical expertise to develop a new antibody against p50. We had seen that commercial antibodies gave identical staining patterns in wildtype and NFkB1-/- (p50) knockout mice, so he attempted to generate an antibody that he thought might work selectively in mice. Commercial antibodies are made against human epitopes, so he looked for an antigenic region that might be fairly unique for mouse, in hopes that some of the nonselectivity seen with the other antibodies might disappear. He contracted AnaSpec to make an N-terminally directed antibody based on the mouse p50 sequence MADDDPYGTGQMFHLNTAL. The antibody was made against the first 14 amino acids, and he tried it in mouse in a hippocampal kainate seizure model. The antibody showed some specific staining at 3-days survival, but a nearly identical pattern was seen in brains from NFkB1-/- mice. The custom-made p50 antibody (NIPB) showed low-level background staining of neurons and a pattern of perinuclear intense staining in cortical neurons after 2-day survival. The stained neurons were in the same locations as dying neurons, as assessed by fluorojade staining. The antibody did not show altered patterns of staining in vitro however, following 10-μM glutamate application. Western blot analysis showed that the predominant bands of staining were at around 40 and 50 kDa, and it appeared identically in WT and KO brains, spleens (strongest), and livers (almost absent). In contrast, the Abcam #7971 p50 antibody showed a band at about 52 kDa in spleen and liver but only very weakly in brain, and it was absent in these areas in the KO tissues.

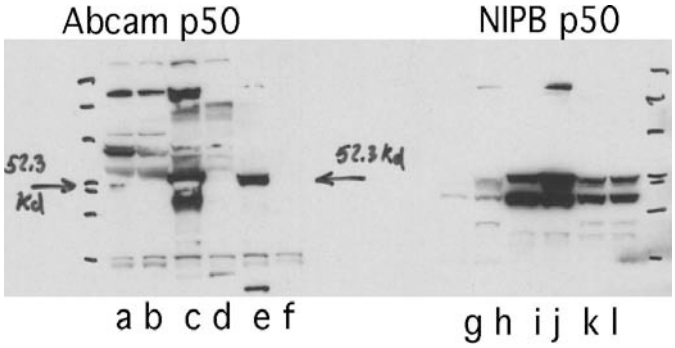

Figure 3. Western blot of whole brain extracts from WT (a,c,e,g,i,j) or p50 KO (b,d,f,h,j,l) mice. Tissues are hippocampus (a,b,k,l), spleen (c,d,i,j), and liver e,f,g,h).

The ability of the Abcam p50 antibody to show differential activity in WT vs. p50 KO brain prompted a more thorough examination in vivo. We employed both the intrahippocampal kainate (KA) and the intrastriatal quinolinate (QA) models, which have been used in publications showing evidence of CNS NF-κB activity. In WT rats, 12 h after QA, the area around the neurotoxic lesion showed a peculiar addition of stained cells that appeared exclusively in the fascicles. The cells were most likely oligodendroglia, but they could also be white matter microglia reacting to the neurotoxin. This response was not similar to anything expected or published. In NFKB1-/- mice, we applied all of our p50 antibodies, and all showed no obvious differences between their responses to intrahippocampal KA in WT versus p50-deficient mice. Interestingly, the Abcam p50 #7971 antibody strongly stained leukocytes in damaged areas of the cannula track in the KO brain (inset at right). This unexpected result, possibly due to cross reaction with p52, was not pursued.

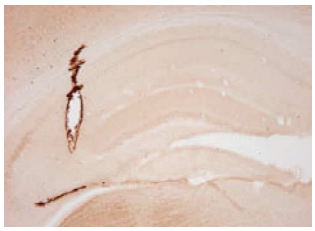

All tested p50 antibodies work identically in immunohistochemistry in wildtype and knockout mice, and we are not using any of these any more

Characterize NF-κB subunit antibodies with Western blotting

All of the antibodies listed in the table were used in Western blots. Some blots were from regional brain extracts taken from mice that were given various challenges such as seizures, and others were untreated mice. Antibodies against the p50 subunit were screened against tissue from NFKB1 (p50) -/- mice. Initially tests were done on brain extracts that were rapidly homogenized and treated with denaturing conditions. Later studies added an initial step in which the freshly dissected tissue was separated into nuclear and cytoplasmic fractions. Quality of separation was determined by routine staining of gels with antibodies to CREB (nuclear) and GAPDH (cytosol). In all cases, rigorous denaturing conditions are applied (boiling for 5 min in reducing agents) to ensure that high molecular weight bands are not protein complexes. Summary of work is given in the Western blot portion of the Appendix

Tracking seizure effects in brain with the phospho-ser276-p65 antibody

We first tried the antibody in the in vivo model of intrahippocampal kainate injection and found that unlike any other NF-κB antibody we had tried, there was a very low level of uniform staining in control tissue and a discretely dark nuclear staining of neurons in areas known to have seizure activity induced by kainate (Figure below). The staining is specific (blocked by the peptide the antibody was raised against) and appropriately localized to cell nuclei where the phosphorylated form of p65 would be expected to reside. The rapid response is consistent with a phosphorylation event. Two other antibodies raised against phospho-ser276-p65 gave similar results (Abcam 30623 and 2615) (not shown). Antibodies raised against phospho-ser536-p65 did not show a specific response (not shown).

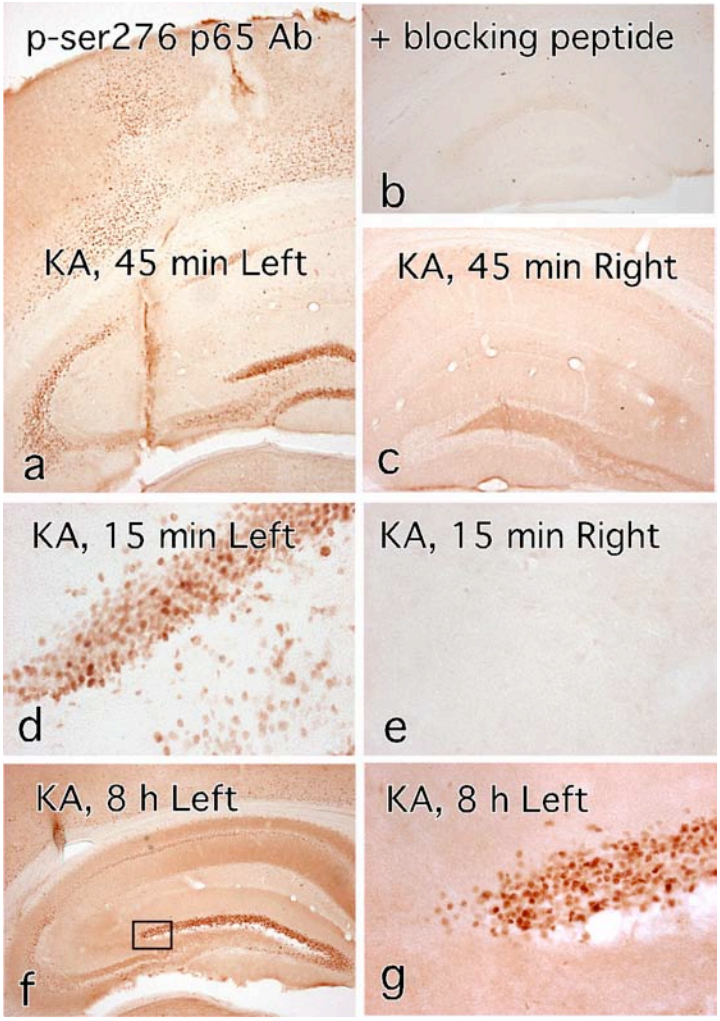

The Cell Signaling #3037 antibody raised against phsopho-ser276-p65 shows faint background staining in control areas of brain (contralateral hipp, c, and dentate gyrus, e). The discretely nuclear neuronal staining appears in areas known to be activated by intrahippocampal kainate injection (a,d,f,g). The response is rapid (15 min) (d) and unilateral (no staining on the contralateral side, shown in c,e) and extends to other areas according to diffusion gradients over time (not shown, but note the cortical staining along the cannula track in a). Some areas still have nuclear staining at 8 h (f,g). Specific staining is completely blocked in the presence of the phosphorylated p65 peptide that the antibody was raised against (b).

A similar kind of rapid response was seen in brain sections from animals given pentylenetetrazol (PTZ) seizures (Figure below). Staining at 30 min after PTZ was widespread and bilateral in the neocortex, predominantly in layers II and III, and it was also present in the hippocampus and striatum. PTZ was selected as the seizure-inducing event because it causes minimal neurodegeneration at later time points.

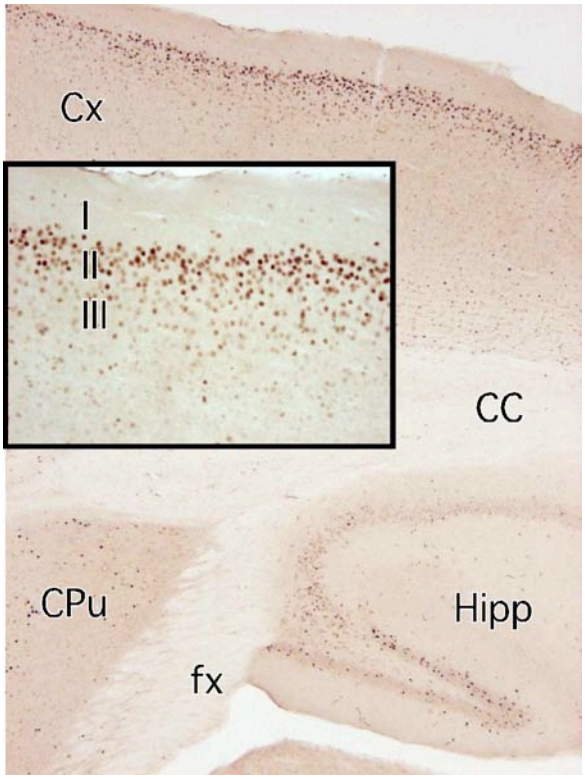

The phospho-ser276-p65 #3037 antibody stains neuronal nuclei in seizure-responsive cortical neurons after i.p. PTZ administration. The laminar pattern of cortical labeling—strong in layers II/III and present also in neurons of layers V/VI—closely matches patterns of activation we showed for Activin A and BDNF mRNA after kindling-induced seizures (1). Similar patterns of activation were found also in the hippocampus (shown) and amygdala (not shown).

Similar successes were achieved when this antibody was applied to hippocampal neurons in culture given glutamate. As shown in the Appendix on cell culture, immunohistochemistry of cell cultures showed that nuclear staining appeared in neurons following low or high-dose glutamate administration, and it appeared as early as immediately after a 10-min application. The same kinds of responses could be recorded in nuclear extracts exposed to Western blots. However, the Western blots revealed that this antibody (and others raised against the same epitope) also stained other proteins from hippocampal or neocortical neurons, and several high-molecular weight bands in particular were typically more responsive to glutamate treatment than the band at the approximate weight of ser276 phospho-p65. We have not found a way to demonstrate that the responses we are measuring by immunohistochemistry are due to antibody binding to the low molecular weight band or to the high molecular weight protein. An effort is underway to identify the large protein that binds the phospho p65 antibody. In the meantime, we are interpreting the immunohistochemical data with great caution.

Western blot summary of work

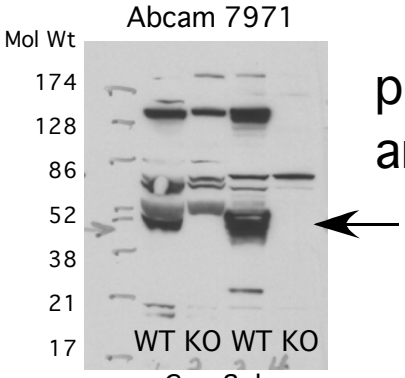

p50 antibodies

The Abcam antibody marks p50 (note band missing in the p50 KO), but it also marks many nonspecific bands.

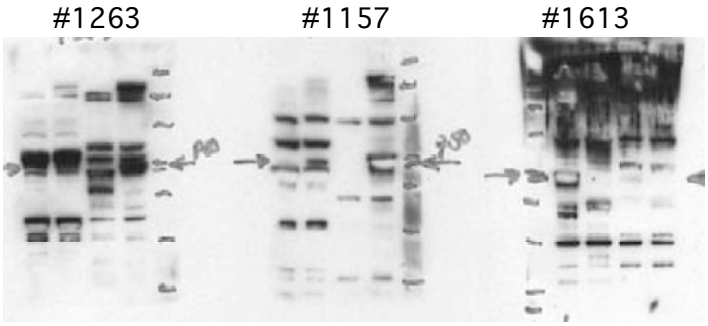

Three NCI p50 antibodies showed no specific pattern in spleen o brain extracts and no specific difference between WY and p50 KO tissue. Lanes 1,2=spleen; 3,4=brain; 1,3= WT; 2,4=p50 KO. SC-8414 antibody marks many nonspecific bands; no difference between WT and p50 found (not shown).

p65 antibodies

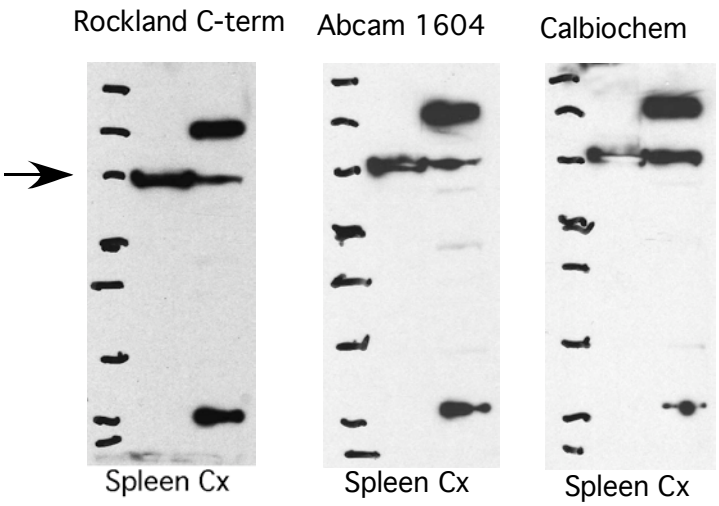

These 3 antibodies are probably the same; they mark one band in spleen and 3 bands in cortex whole cell extracts.

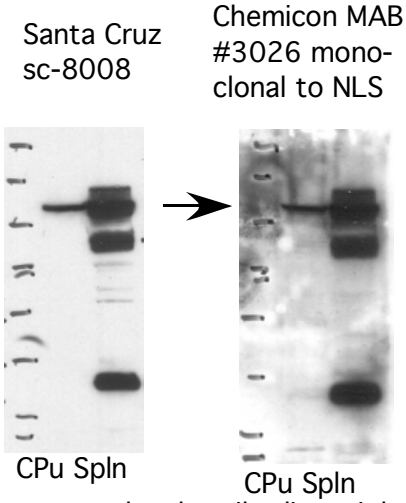

These two monoclonal antibodies might be the same; they mark one band in striatal whole cell extracts, and appear lower in intensity but more specific in striatum than spleen.

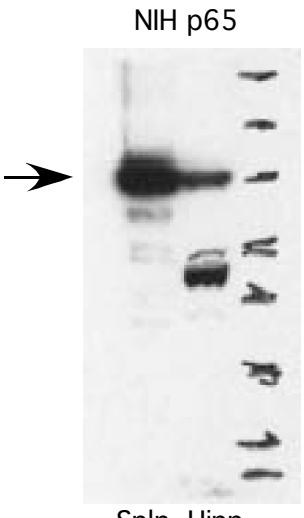

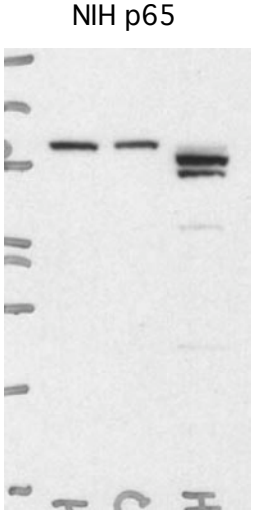

NIH p65 antibody shows a doublet in cells. When samples were separated into cytosolic (C) and nuclear (N) fractions, the doublet appeared in the nucleus. Typically there was no strong response to treatments

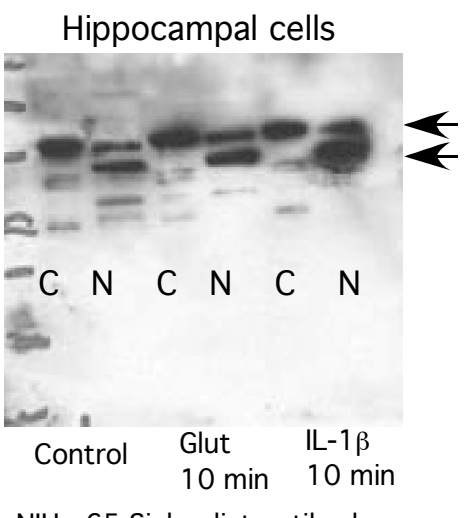

NIH p65 Siebenlist antibody

NIH p65

CS3037 p65 phosphorylated at ser276

Mouse hippocampal neurons

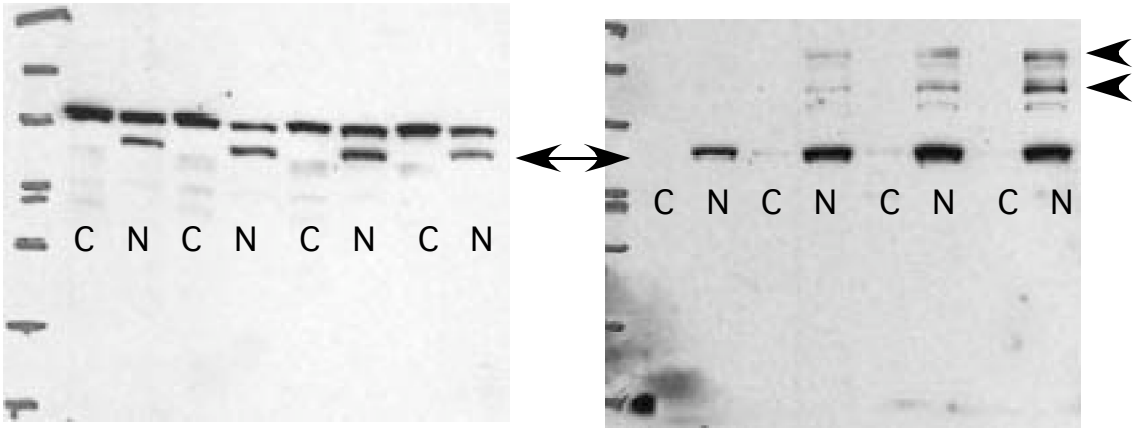

Control | Glut 10 min | IL-1 10 min | IL-1 1 h

Control | Glut 10 min | IL-1 10 min | IL-1 1 h

When control PO4-p65 (Ser276) levels are reduced, then an increase in nuclear PO4-p65 (S276) and a decrease in nuclear p65 can be shown. The size of the PO4-p65 band is the same as the size of the smaller p65 band. With the #3037 antibody, stimulation induces bands at very large molecular weights (arrowheads).

CS3037 p65 phosphorylated at ser276

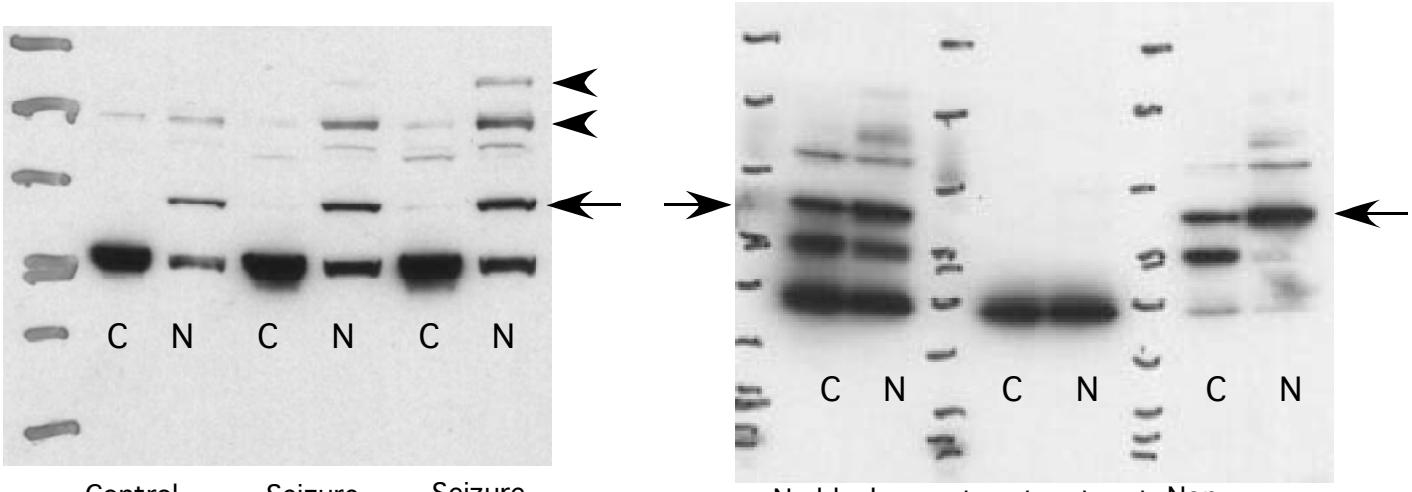

Control | Seizure brain #1 | Seizure brain #2

No block | phosphorylated peptide block | Non-phosphorylated peptide block

After PTZ-induced seizures, the PO4-p65 band increases slightly in prefrontal cortex (shown) and hippocampus, but not cerebellum (not shown). Low-molecular weight bands appear inconsistently, and high molecular weight bands (arrowheads) may be seizure induced.

The band at approximately 65 kDa is blocked when the brain (hipp) extracts are incubated with the phosphorylated peptide of the same sequence but not with the non-phosphoryalted peptide of the same sequence as the peptide that the antibody was raised against. Note that other bands are blocked too, notably the high molecular weight bands.

Cortical neurons.
EGTA decreases basal cell activity, and stimulation by glutamate of PO4-p65 (S276) seen. Similar results were obtained with the antibody against phospho-CREB. In addition, a high molecular weight protein is strongly stimulated, and it appears in neurons in culture and in nuclear fractions from brain tissues subjected to seizures.

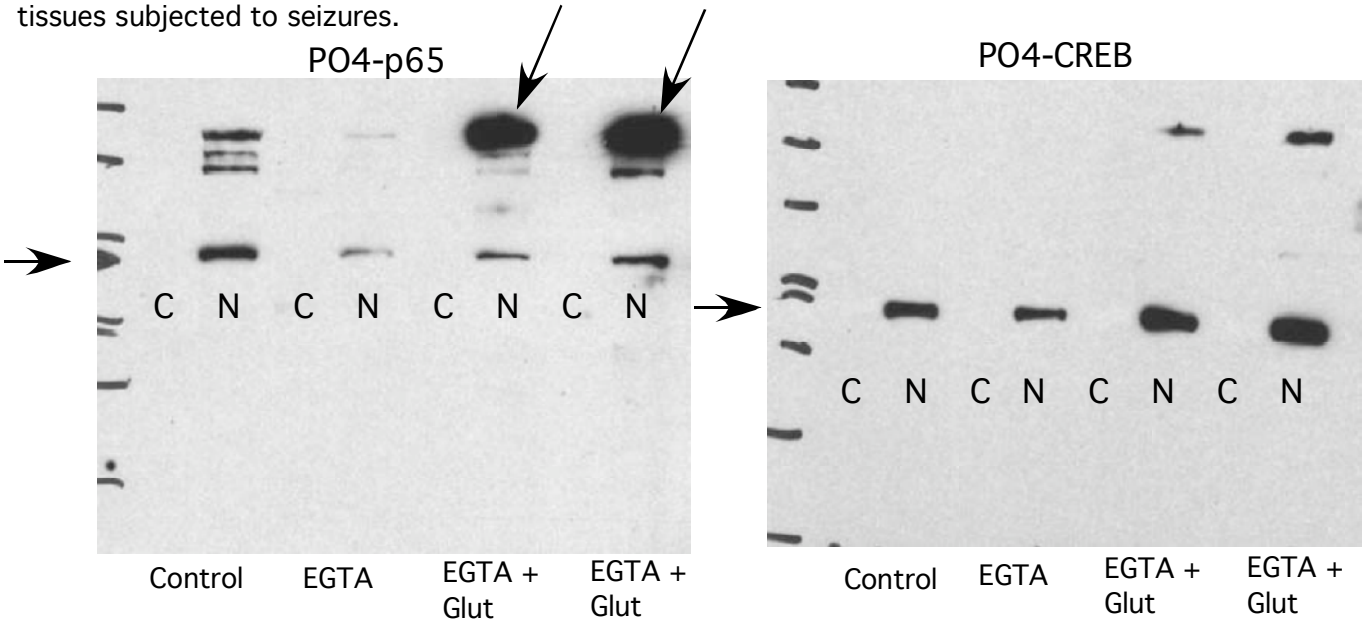

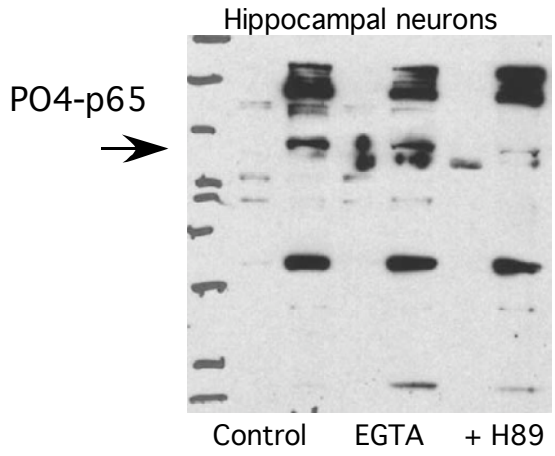

H89 reduced the basal signal in some experiments, but it only occasionally blocked the Glutamate-induced signal (not shown). Other treatments that had inconsistent or negative effects were treatment with APV and glutamate receptor blockers,

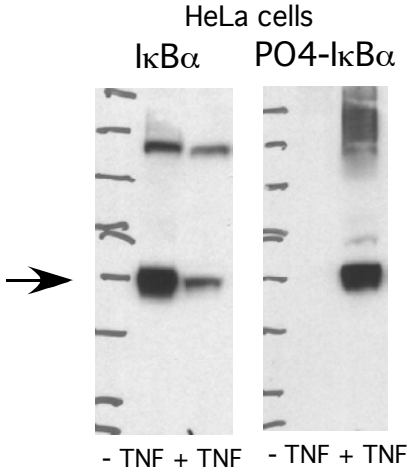

IκBα disappears from HeLa cells after TNFα administration. Phosphorylated IκBα (ser 32) appears upon stimulation. Cell Signaling antibodies #9246, #9242, and #2859 used.

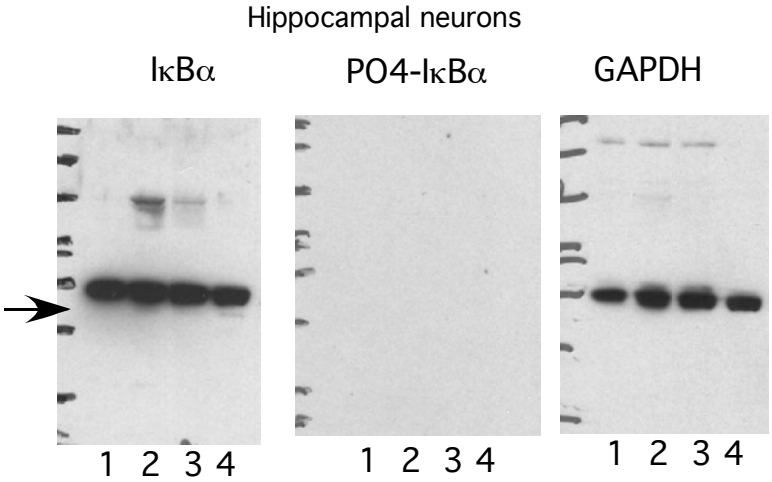

Hippocampal neurons are unresponsive (measured by IkB and phosphorylated IkB levels) after treatment with 10 nM PMA (lane 2), 20 μM forskolin (lane 3), or 100 μM glutamate (lane 4). GAPDH shows loading control. The same antibodies show expected changes after TNFα stimulation in HeLa cells (left)

Additional control studies

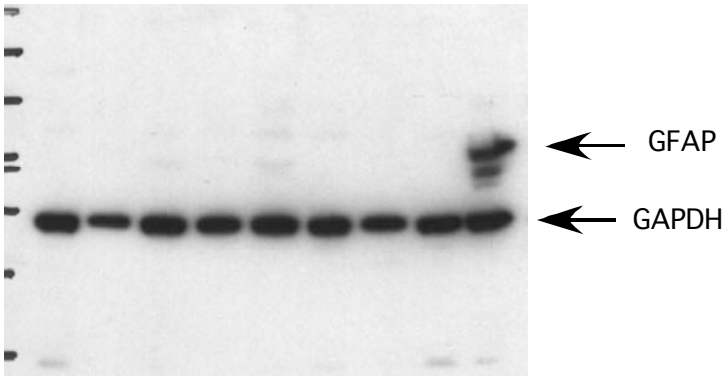

Samples of cytosolic extracts from numerous different experiments using mouse hippocampal or cortical neurons show undetectable levels (8 lanes on the left) compared with strong band in cultured astrocytes (right lane).

CS3037 PO4-p65 antibody

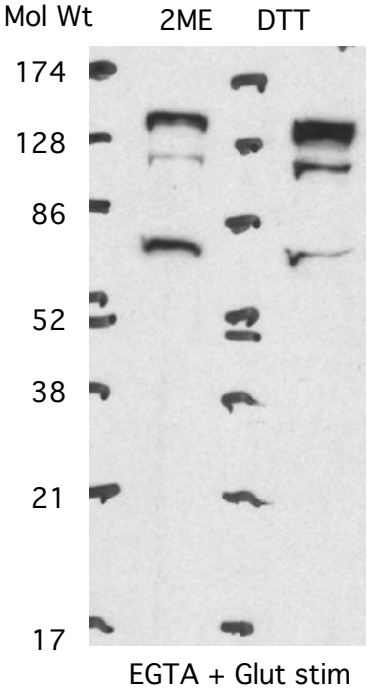

The phospho-ser276-p65 antibody stains multiple bands in neurons and brain tissue. The large molecular weight bands appearing at around 130 kDa are blocked by the corresponding phosphorylated but not unphosphorylated) peptide that the antibody was raised against. These bands are the most dramatically induced by glutamate in neurons and by seizures in extracts from cortex or hippocampus. We wondered if the band might be a multimeric complex (i.e., heterodimers or homodimers of p65 that are not dissociated by the denaturing conditions). Samples were boiled for 5 min in SDS to break protein-protein interactions, and that did not alter the appearance of the big band. Two reducing agents were used, dithiothreitol (DTT) and β-Mercaptoethanol (2ME). The result is that the large band is still present.

EMSA analyses

Nuclear extracts from Spleen (untreated)

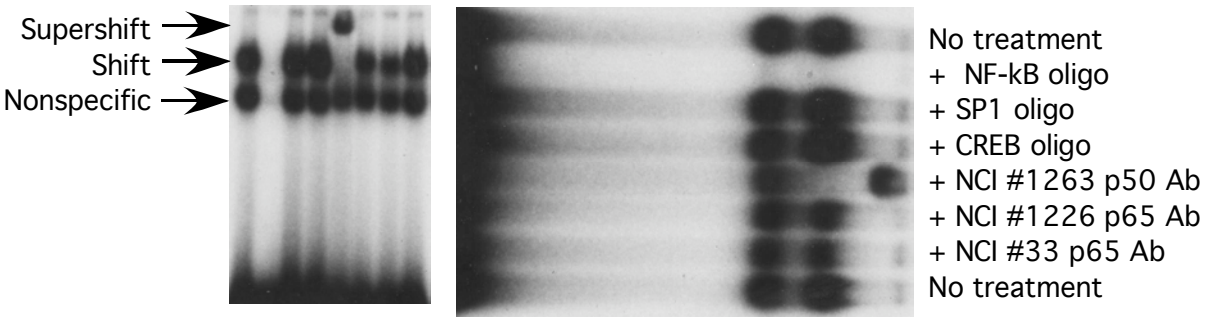

Nuclear extracts from spleen bind the canonical radiolabeled kB oligo (5'-AGTTGAGGGGACTTTCCCAGGC-3') as revealed in the specific shift that occurs just above a nonspecific shift. The shifted band is completely inhibited by cold kB oligo but unaltered by SP1 or CREB oligos. It is strongly supershifted by an NCI p50 antibody (#1263), and its intensity is diminished by two NCI p65 antibodies.

Nuclear extracts from neocortical neurons in culture

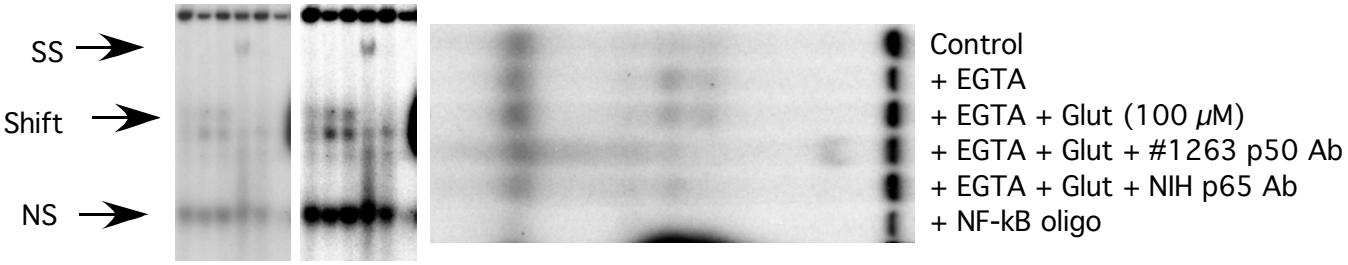

Nuclear extracts from cultured neurons show weak but measurable specific kB oligo binding that is enhanced by glutamate treatment and supershifted by p50 and p65 antibodies. The effect is clearer when the image is contrast enhanced.

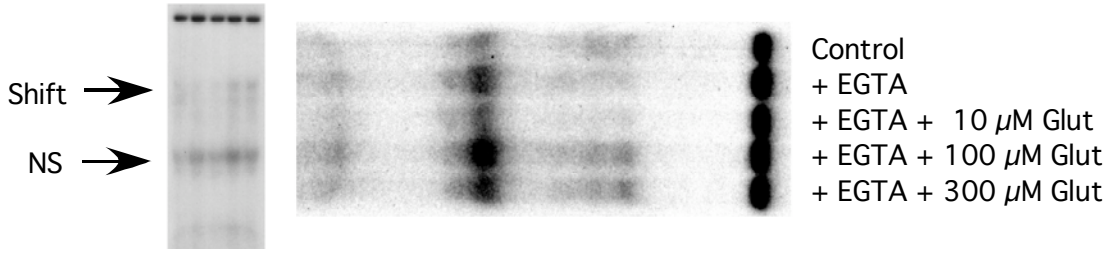

Glutamate dose-dependently increases specific kB oligo binding in nuclear extracts from hippocampal neurons.

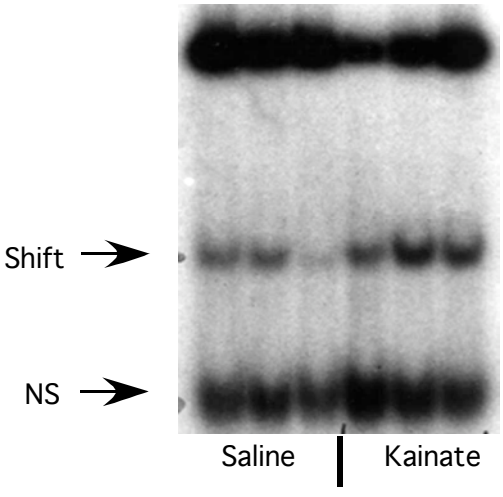

Nuclear extracts from mouse neocortex taken 3 hours after kainate seizures (n = 3) or saline (n = 3).

Kainate seizures increase neocortical kB oligo binding.

Western Blot Protocol

Prepare appropriate cellular extract for analysis (Cytoplasmic, Nuclear or Whole Cell Extract)
Measure protein content of each sample (use the Bradford Method, be consistent in this measurement as all sample results are dependent on the relative precision of this determination.)

Gel System (This can vary depending on the user's preference). In our case:

- 10% Bis-Tris (Invitrogen NuPAGE-SDS) mini-Gels (1.0 mm X 10 Well)
- using 1 X MOPS-SDS Running Buffer
- Prior to loading on the SDS gels, add to all samples in a microcentrifuge tube: (for 20 uL total volume):
- 5 uL 4X Loading buffer (0.25 M Tris pH 8.0, 8% SDS, 40% Glycecrol, Bromphenol Blue Dye)
- 2 uL 10X DTT (500 mM)
- up to 13 uL of sample + H2O
- (Sample load: 5 – 20 ug protein per well.)
- Boil 5 min, vortex, briefly spin to collect all the sample at the bottom of the microcentrifuge tube then load onto the gel.
- (Note: Add Pre-stained protein ladder to lane 1 for relative Molecular weight markers and sample orientation)

Run gel approximately one hour at 200 volts using 1 X MOPS-SDS Running buffer.

Transfer Proteins to Membrane:

- Prepare transfer buffer solution (100 mL 10X tris-glycine Transblot buffer, 200 mL 100% MeOH, dH2O to 1 L)
- Pre-wet PVDF membrane (Millipore Immobilon P) in 100% MeOH, then soak in transfer buffer
- Pre-soak transfer sponges and Whatman paper in transfer buffer.
- Assemble transfer apparatus with buffer, gel, membrane and sponges according to manufacturer's instructions.
- Transfer proteins to membrane for 2 hours at 40 volts.

Blocking and Antiserum Incubations:

- Remove membrane from transfer apparatus, examine membrane for transfer of Pre-stained Protein Molecular weight markers
- Block membrane for two hours in 5% dried milk/Tris-Buffered-Saline-0.05% Tween20 with gentle shaking at room temp.
- Add appropriate primary antiserum (Dilution of antiserum to use varies depending on the antiserum and the amount of protein loaded on the gel. The dilutions can range from 1:300 to 1:3000, only experience with a particular antiserum can best determine the primary dilution to use, therefore, try an intermediate dilution and adjust accordingly.)
- Incubate the membrane and the primary antiserum in 5% dried milk/Tris-Buffered-Saline-0.05% Tween20 at 4 degrees centigrade overnight with gentle shaking.
- After the overnight incubation, wash the membrane 3 times at room temperature for 10 min each with Tris-Buffered-Saline-0.05% Tween20.
- Add secondary antiserum, usually goat anti-rabbit IgG-HRP (or anti-mouse if the primary was a mouse monoclonal), diluted in 5% dried milk/Tris-Buffered-Saline-0.05% Tween20 and incubate for 1-4 hours (depending on secondary antiserum dilution, example, 4 hours at a dilution of 1:20,000) at room temperature with gentle shaking.
- After the secondary antiserum incubation, wash the membrane 3 times at room temperature for 10 min each with Tris-Buffered-Saline-0.05% Tween20.
- Detect the antiserum signal using a chemiluminescent substrate: West Duro (Pierce) for lower protein expression, or West Pico (Pierce) if protein levels are high enough and expose to X-ray film. (Biomax MS film for greater sensitivity to a lesser protein expression signal or Biomax MR film for a clearer signal to a higher expressed protein signal)

The blots can be re-blotted with the following antisera to serve as protein loading controls.
For a Cytosolic or Whole Cell loading control, GAPDH antiserum (SC25778) can be used at a dilution of 1:2000- 1:5000. For a Nuclear loading control, CREB1 antiserum (SC58) can be used at a dilution of 1:1000.

EMSA Protocol

Pour Acrylamide Gel:

1. Assemble Plates, spacers, and clamps.
2. Pour 6% acrylamide Gel (non-denaturing)

H_2O	34.5 mL
10x TBE	2.5 mL
30% Acrylamide/Bis Soln	10.0 mL
50% Glycerol	2.5 mL
10% APS	450 uL

mix well while minimizing bubble formation. Add 50 uL TEMED. Mix and pour, add combs. Gel will take approx. 15-30 min to polymerize. After polymerization, gel can be wrapped in Saran Wrap and stored at 4°C.

10x Binding Buffer:

Composition

100 mM Tris HCl (pH 7.4)
200 mM KCl
5 mM EDTA
10 mM MgCl2
25 % glycerol (v/v)

Additives:

1 ug poly dI-dC
20 ug BSA
0.5% NP40

PER 20 uL BINDING RXN:

2ul 10X Binding Buffer
2.5 ul Additives
up to 14.5 uL Sample + H20

1uL of 32P-labeled dsOLIGO probe (approx. 50,000 CPM)
1uL cold competitor (if needed)
or 1 uL specific antiserum for supershift (if needed)

If no competitor or antiserum is to be used, add labeled probe and incubate 30 min. at room temp. If antibody or competitor is to be used, pre-incubate for 10 min at room temperature with competitor or antiserum, then add labeled probe and continue the room temperature incubation for 30 min.

While binding reaction is incubating, pre-run polyacrylamide gel at 200V, 30 min, using 0.5xTBE as running buffer. Flush debris out of individual sample loading wells.

Run samples on acrylamide gel 3-4 hours at 200V.

Dry the Gel (Optional)

Transfer the gel to Whatman Paper (mark first well). Cover top of gel with Saran Wrap and dry at 80°C in vacuum dryer 1-2 hour. Or, transfer the gel to Whatman paper (mark first well) and place gel inside sealable plastic bag. Scan with Pancake Counter to determine strength of radioactive signal.

Expose the Gel

Place gel in cassette. Add BIOMAX MS (maximum sensitivity) X-Ray film, intensifying screen and place in -80°C freezer for film exposure (exposure time varies depending on strength of signal).

Probes used

The consensus sequence kB, SP1 and CREB double stranded Oligos were supplied with Promega's Gel Shift system (i.e., kit). Their sequences on the plus strand are as follows (shown as a single strand, but the oligo used is double stranded)

κB: 5'-AGTTGAGGGGACTTTCCCAGGC-3'
SP1: 5'-ATTCGATCGGGGCGGGGCGAGC-3'
CREB: 5'-AGAGATTGCCTGACGTCAGAGAGCTAG-3'

Cytosol-nuclear fraction preparation:

LOW SALT BUFFER:

10 mM TRIS, pH 8.0
1.5 mM MgCl(2)
10 mM KCL

10 % NP40:

10 % NP40 (IGEPAL CA-630) in dH2O

HIGH SALT BUFFER:

20 mM TRIS, pH 8.0
1.5 mM MgCl(2)
25% Glycerol
0.2 mM EDTA
0.42M NaCl

INHIBITORS+ (100x ea):

(Store at 4 degrees, remove to room temperature just prior to use)

Phosphatase Inhibitor Cocktail 1 (Sigma #P2850-1 ml)
HALT Protease Inhibitor Cocktail (Pierce #185566)
Add fresh to both Low and High Salt Buffers, just prior to use

PROCEDURE:

KEEP ALL BUFFERS AND HOMOGENIZERS ON ICE

(Note: For use with mouse **tissues)**

1. Homogenize tissue (example, the size of mouse Hippocampus, if larger, scale up amount of buffers used) in 0.2 ml of Low Salt Buffer using 8-10 strokes of a Dounce glass homogenizer on ice.
2. Transfer to pre-labeled microcentrifuge tube, vortex 10-15 seconds and let sit on ice 10 min.
3. Add 1/10 volume of 10 % NP40 to bring the final NP40 concentration to 1%
4. Vortex for 5-10 seconds, wait 1 minute, re-vortex 5-10 seconds and spin IMMEDIATELY at maximum speed in a pre-chilled (4°C) microcentrifuge for 5 min.
5. Carefully remove most of the supernatant and transfer to a tube labeled: CYTOSOL, then carefully remove any remaining liquid from the pellet, SAVE the pellet and discard this extra liquid.
6. To the remaining pellet (Nuclei, membranes and cell debris) add 100 ul High Salt Buffer, resuspend the pellet by vortexing 15-20 seconds.
7. Keep the tube on ice for a total of 45-60 min, vortexing every 10 min for 15-20 seconds.
8. Spin the sample at 4 degrees for 15 min at maximum speed.
9. Remove the supernatant, the Nuclear extract fraction, to a pre-labeled tube and store at -80°C for later analysis. Discard the pellet (now only cell debris).
10. Determine protein concentrations on both Cytosol and Nuclear fractions for later Western Blots.

For use with Neuronal Cell Culture:

The NE-PER (Pierce), Nuclear and cytoplasmic extract preparation kit was used according to the manufacturer's instructions.

Ribonucleotide probe generation and ISHH protocol

RNA Isolation: Tissue (brain and spleen) was collected and stored in RNAlater. Tissue was subsequently homogenized on ice in TRIzol (1 mL per 50-100 mg of tissue) in RNase-free Eppendorf tubes. Samples were incubated at RT for 5 min, treated with chloroform (0.2 mL per 1 mL TRIzol), and spun in a microcentrifuge to separate out the RNA. The RNA (the upper, aqueous phase) was transferred to a fresh tube, and precipitated out using isopropyl alcohol (0.5 mL per 1 mL TRIzol used to homogenize). Samples were incubated at RT for 10 min, then spun down for 10 min at 12,500 rpm to pellet the RNA. The pellet was then subsequently washed in 75% ethanol and allowed to air-dry before being resuspended in RNase-free water. The RNA was then analyzed using a Nanodrop spectrophotometer to confirm quality and identify concentration. Samples were stored at -20°C.

Reverse Transcription of RNA to cDNA using SuperScript cDNA First Strand Synthesis Kit (Invitrogen): 1 ul 50 uM Oligo $(dT)_{20}$ and 1 ul Annealing Buffer was added to standarized concentrations of RNA from each sample and brought up to a total volume of 10 ul in ultra pure water in RNase-free PCR tubes. Tubes were incubated in a thermal cycler at 65°C for 5 min, then immediately held on ice for 1 minute. 10 ul 2X First-Strand Reaction Mix and 2 ul SuperScript III/RNaseOUT Enzyme Mix were added to each tube. The tubes were then incubated for 50 min at 50°C. The reaction was terminated at 85°C for 5 min, chilled on ice, and stored at -20°C.

PCR Amplification of cDNA using Transgene Specific Primers: Primers were identified using sequence data from the literature in conjunction with GENBANK and BLAST. Primers were generated using Primer3. 1 ul of each primer (20 uM, Sigma) was combined with 2 ul cDNA, added to 46 ul PCR Supermix, and run on a block PCR

PCR product was then run on a 1% agarose gel (.4 mg agarose in 40 mL 1xTBE + 4 ul EtBr) at 100V for 1 hr, and the amplified band was excised for subsequent product purification. The desired PCR product was then extracted from the gel bands using a Qiagen MinElute Gel Extraction Kit.

Ligation of PCR Product into Vector & Transformation of Competent Cells: 4 ul purified PCR product was added to 1 ul TOPO Vector (Invitrogen) and incubated at RT for 15 min. 2 ul of this TOPO cloning reaction was then added to a vial of OneShot cells and incubated on ice for 30 min. Immediately following, cells were heat-shocked for 1 minute at 42°C, transferred to ice for 2 min, placed in 250 ul of SOC medium and incubated at 37°C with shaking for one hour. Cells were then plated on X-GAL + IPTG + Ampicillin pre-treated plates and grown overnight at 37°C.

Colonies were selected using lacZ gene disruption (colonies appear white, as opposed to blue) as an indicator of plasmid insertion. Colonies were grown up individually in 5 mL LB Broth (10% Ampicillin) O/N at 37 C with shaking.

Plasmid Isolation and Sequencing: Plasmids were isolated from 2 mL O/N culture using a Qiagen Miniprep Kit. 1 mL of culture was stored in a 15% glycerol stock at -80°C.

Plasmids were linearized using ECO RI to release the insert. Linearization product was run out on a 1% agarose gel to confirm the presence of the correct sequence. Plasmids containing the insert were sent to the NINDS Sequencing Facility for sequencing to verify ligation and ascertain direction of insertion.

Plasmid Linearization for Probe Template: Remaining isolated plasmid was linearized using ECO RV and SpeI to generate sense and antisense templates. 5 ul of linearized DNA was run on a 1% agarose gel to confirm successful linearization.

^{35}S Riboprobe Transcription: 3 ul 5X transcription buffer, 1.5 ul 100 mM DTT, 0.3 ul RNAsin (40 U/ul), 2.75 ul ΔNTP, 0.5 ul DNA (1 ug/ul), 7.5 ul [^{35}S]UTP (50 uCi), and 0.5 ul RNA polymerase (T7 or SP6) were combined in an RNase-free 1.5 ul Eppendorf tube and incubated at 37 C for 1.5 hours (0.5 ul additional RNA Polymerase was added half way through the incubation). 7.5 ul Sterile DEPC-H_20, 0.5 RNAsin, and 0.5 ul RQ1 DNAse were added, and the reaction was incubated for an additional 10 min. The reaction was purified using a ProbeQuant Micro Column (Pharmacia Biotech) to remove unincorporated NTPs. 1 ul 5M DTT was added to each tube. 1 ul of each probe was counted in 10 mL Cytoscint using a liquid scintillation counter.

Tissue Preparation: Fresh frozen brain and spleen tissue was sectioned in a cryostat to obtain 10 µm-thick slide mounted sections. Tissue was brought to room temperature, fixed for 5 min in 4% formaldehyde in 1xPBS (pH 7.5), and rinsed in 1xPBS (twice). Tissue was rinsed in TEA-HCL then acetylated in TEA-HCl/acetic anhydride (made fresh) for 10 min. Tissue was rinsed in 2X SSC then dehydrated/delipidated in ethanol washes (70% for 1 minute, 80% for 1 minute, 95% for 2 min, 100% for

1 minute) and chloroform (for 5 min). Slides were rinsed in 100% EtOH for 1 minute and 95% EtOH for 1 minute and allowed to air dry.
Riboprobe Hybridization: Riboprobe was combined with riboprobe hybridization buffer (25 ul hybridization buffer per 1,000,000 cpm), heat denatured at 90°C for 5 min, and chilled on ice for 5 min. Mix was brought to room temperature and formamide (0.5 x total volume), 10% SDS (0.01 x total volume), 10% Na thiosulfate (0.01 x total volume), and 5 M DTT (0.02 x total volume) were added. 50 ul HB mixture was applied to each slide, covered with a 24x30 coverslip, and incubated overnight at 55°C in the presence of 4X SSC/50% formamide to prevent evaporation.
Slide Washes: Coverslips were removed the next day and slides were incubated for 30 min in RNase A in RNase buffer to removed non-hybridized probe. Slides were washed in 2X SSC at room temperature, then in 2X SSC at 50°C for 1 hour, 0.2X SSC at 55°C for 1 hour, and 0.2X SSC at 60°C for 1 hour. Tissue was dehydrated in 50%, 70%, 80%, and 90% EtOH with 0.3M NH_4OAc, then in 100% EtOH for 1 min each. Slides were allowed to air dry, then placed on film. Exposures ranged from 1 to 5 days.

Microarray, qRT-PCR analysis

Forebrain tissue was collected from adult male WT and NFkB1-/- mice 60 min after IP injection with SAL vehicle or 0.1mg/kg LPS (n=6 per group). Tissue samples were disrupted and homogenized by passing tissue and 1 ml Trizol (Invitrogen) through a 25-gauge needle, attached to a sterile plastic syringe. RNA was precipitated and purified using a modified protocol from the Qiagen RNeasy Kit. Briefly, 200 µl chloroform was added to tissue lysate, samples were then mixed and centrifuged and the aqueous phase was transferred to a new tube. To the aqueous phase, 200 µl of 100% Ethanol was added and the solution was then transferred to a Qiagen RNeasy column. The RNA was then cleaned and concentrated with the Qiagen RNeasy Micro Kit that included a DNase digestion according to the manufacturer's recommended procedure. RNA concentration and quality were determined by UV absorbance (NanoDrop) and ribosomal RNA integrity (Agilent 2100 Bioanalyzer).

RNA biotin-labeling and hybridization procedure was performed through the core Microarray Facility at National Human Genome Research Institute (NHGRI) at the NIH (Bethesda, MD) and is available at http://research.nhgri.nih.gov/ma/protocols.shtml

Measurement of data and specifications
Arrays were scanned with the GeneChip Scanner 3000 7G. GeneChip Operating Software (GCOS, Affymetrix) was used for initial processing of the scanner data, including generation of cel files that were used for computation of GCRMA gene expression scores with GeneSifter software. The GCRMA procedure involved quantile normalization, and was described by Wu et al. (2004) (www.bepress.com/jhubiostat/paper1 <http://www.bepress.com/jhubiostat/paper1>).

Array design
The Qiagen Mouse Genome Oligo Set Version 3.0 arrays were printed on site at NHGRI. The array provided comprehensive coverage of the transcribed mouse genome on a single array analyzing 24,878 unique genes and 32,829 gene transcripts through 31,769 70mer probes. The oligonucleotide sequences, their locations on the array, and other annotations are available in files that can be viewed at http://research.nhgri.nih.gov/ma/mouse_v301_genelist.html.

qRT-PCR
Quantitative RT-PCR was performed to validate microarray data of selected genes. For each sample, 2.2 µg RNA was reverse transcribed using SuperScript III reverse transcriptase (Invitrogen) as per manufacturers directions. Real-time PCR was performed using 2x SYBR Green PCR Master Mix and detected by a BioRad iCycler (BioRad). Universal thermal cycling conditions were as follows: 10 min at 95 °C, 40 cycles of denaturation at 95 °C for 15 sec, and annealing and extension at 60 °C for 1 min. All reactions were performed in triplicate and were normalized to GAPDH. Relative differences among treatment groups were determined using the delta delta Ct method as outlined in the Applied Biosystems protocol for RT-PCR. Results are expressed as fold changes in mRNA expression with respect to control groups. Calculations were done assuming that 1 delta Ct equals a 2-fold difference in expression. Significance values were determined using unpaired t-tests.

Genome Alignment and Annotation Database (GALA) Analysis

The GALA database incorporates genomic annotation information with multi-species alignments to allow complex querying on publicly available sequence information. A genome-wide search was performed to detect the presence of NFkB1 p50 homo-dimer preferring sequences, GGGRNTTYCC within -10,000 bp to 100 bp of a known Gene transcription start site (TSS), as listed in the mouse known Gene track of the UCSC genome browser, assembly mm5 (Mouse May 2004). For promoter regions of interest that contain putative NFkB1 p50 homodimer binding sites, sequence information was rechecked against the most recent genome mouse assembly (Ensembl Mouse release 48-Dec 2007).

Genome Alignment and Annotation Database (GALA)
The GALA database incorporates genomic annotation information with multi-species alignments to allow complex querying on publicly available sequence information. A genome wide search was performed to detect the presence of NFkB1 p50 homo-dimer preferring sequences, GGGRNTTYCC (24) within -10,000 bp to 100 bp of a known Gene transcription start site (TSS), as listed in the mouse knownGene track of the UCSC genome browser, assembly mm5 (Mouse May 2004). For promoter regions of interest that contain putative NFkB1 p50 homo-dimer binding sites, sequence information was rechecked against the most recent genome mouse assembly (Ensembl Mouse release 48-Dec 2007). The sequences searched and a single example of an outcome is given below. Hundreds of genes were found to have the sites in the defined upstream regions. The searchable file (not provided) is 32 MB. An example of the query rules and one gene (Creb1) readout is given below:

```
# Update on Feb. 13, 2008

- Expanded search region:  -10kb to 100bp around clusters of TSSs.
- Used GGGRNTTYCC as the consensus sequence.
- Added chromosome coordinates to sequence matches in results file.
- Added chromosome coordinates and sequence match to gene file.
- Changed position from position in FASTA sequence to distance from TSS
cluster.

GGGGATTTCC -> GGAAATCCCC
GGGGCTTTCC -> GGAAAGCCCC
GGGGGTTTCC -> GGAAACCCCC
GGGGTTTTCC -> GGAAAACCCC
GGGGATTCCC -> GGGAATCCCC
GGGGCTTCCC -> GGGAAGCCCC
GGGGGTTCCC -> GGGAACCCCC
GGGGTTTCCC -> GGGAAACCCC
GGGAATTTCC -> GGAAATTCCC
GGGACTTTCC -> GGAAAGTCCC
GGGAGTTTCC -> GGAAACTCCC
GGGATTTTCC -> GGAAAATCCC
GGGAATTCCC -> GGGAATTCCC (palindrome)
GGGACTTCCC -> GGGAAGTCCC
GGGAGTTCCC -> GGGAACTCCC
GGGATTTCCC -> GGGAAATCCC

7188 matches in 5636 genes out of 19319 genes searched
# Original File
Finding NFKB binding sites in promoter regions.
METHOD:
1. Find CAGE tags within -1000 to 100 of a knownGene TSS, as listed in the
mouse knownGene track of the UCSC genome browser, assembly mm5 (Mouse May
2004).  The CAGE tags are from the rikenCageCtssPlus and the
rikenCageCtssMinus tables, which predict gene start sites base on CAGE tag
counts.  These tags form a cluster of alternative transcription start sites
```

around a gene. In some cases, the knownGene track already has listed alternative transcription start sites as separate genes. These are merged and listed together in the results.
For example, the genes X92497, M95106, and AK044993 (CREB1) have start sites near each other and share CAGE tags within the -1000 to 100 range.
Note: an option would be to include results for knownGenes without nearby CAGE tags.
We are assuming that CAGE tags that fall outside the -1000 to 100 range of knownGenes are other forms of transcripts, likely non-coding RNA.
2. Each tag cluster around a gene forms a range on the chromosome (<tagDownstream> to <tagUpstream>). We define the promoter region as 1000 bps upstream and 100 bps downstream of the transcription start site. Since the start site is range, we define the promoter region as 1000 bps upstream and 100 bps downstream of the CAGE tag ranges. Therefore, the promoter region becomes <tagDownstream>-1000 to <tagUpstream>+100.
3. Search for the consensus sequences (as well as reverse complement) within each of defined regions.

RESULTS:
The results are in file roughly in a FASTA format as follows. Each gene with one or more of the consensus sequences in its promoter are listed. An example follows. The first line is in FASTA format, listing chromosomal location, strand, and UCSC identifiers (mRNA ids) for the gene. Next is the list of matching consensus sequences with the sequences position in the chromosome range. In the example, GGGAATCCCC matches at position 948, which would be at chr1:64,933,549. The next line lists the number of matching consensus sequences in this gene. Other information for each transcript (different mRNA ids) is then listed as follows:
- SWISS-PROT: protein Accession number and display ID
- Gene Symbol
- RefSeqId and NCBI protein Accession number
- a description

Finally, the entire sequence with repeats in lower case is shown. The consensus sequence is marked by * beneath it. The end of the upstream promoter region is marked by P (position 1000) and the most downstream transcription start site is marked with an S.

```
>chr1:64932601-64934207 +     X92497,M95106,AK044993
GGGAATCCCC 948
FOUND 1
X92497
   SWISS-PROT:  Q62347 Q62347
   Gene Symbol:  Creb1
   RefSeq ID:  NM_009952,  NCBI protein Accession number:  NP_034082
   description:  Transcription factor/DNA binding protein.
M95106
   SWISS-PROT:  Q01147 CREB_MOUSE
   Gene Symbol:  Creb1
   RefSeq ID:  NM_009952,  NCBI protein Accession number:  NP_034082
   description:  cAMP response element binding protein (CREB).
AK044993
   SWISS-PROT:  BAC32174 BAC32174
   Gene Symbol:  Creb1
   RefSeq ID:  NM_009952,  NCBI protein Accession number:  NP_034082
   description:  9.5 days embryo parthenogenote cDNA
GCCACTGCAAATGGAGAGAGACAGTAAAAGACAGGTGGAACTCGGAAAGG
AGCTTAAGGAGGAAGTTTCTATATTTTATTTATTGCCcacacatactact
gtgatgtaagtgctgaggtcaaaggacaacttatgggagctggttctctc
cttctaccacgtgggttctcgaaattgaccttagattatctggcttggtg
```

```
gcaagggcctttattcaTCTCACCAATGCCACAAGAGTCTTCTTAAAGAG
AGGAAGAGACGTTAGCATGCTAAAAGTTCTGGTTAGAAACAAAAGAAAAT
TAAGCTACTCTTCAGTATAATGTCCTTGGGAAAGCGGGAACGGCTAGGAC
ACACGGAATGAAGGCAAGCTCAGTGTTATAAAACGTCAACAAGGGCTGGC
GTCCAGCAGGAACAAAACTATAGGAAGAGGGCTGAACGGCACAACAACAA
AAGGTGAAGAACTGGCGGTTAGGGGCAACTCAGAGAGCAGTTGCGGTAGC
TTTGAGGCTACGGAAGTCACACTGTCAAGTTCTGGGGTGCAAACGGTGGA
AGCCACGCCGCAGCAGCGTGCCACCGCTGCAGAAAGGGCTGAGAAAAGTC
AGCACAGGATGTCGCGGGCAGGTAGGGTGGGGATCTGTTTCAAGTGTTGA
GAGCAGCATGGCTGATCATTTCTCCAGCCTCAGAGGGAGGACGGTACCCA
GTACCTAGGGGCTCTGGCTGGCCGCAAAGCGGAGCTGAATCCCCACATGC
CACCTGTGCCATAGCTTTCTTCCCAGCAAAGAACCAGCTCCGGCCCGGCA
GACTCCCCTGGCCGGTAGCCGGCGTCTCCAACCTTCCAGCGCCGTCCGCG
CGGCTCTGGGCCCTCGCGGCGCGTCAAAGTTCCCGGGCGGTCTGCTTCCG
CCGCAGGATCAGACCGCGCGGGGGTTTCCAGCAAGTCCCCGCCACCCCGG
                                                    **
GAATCCCCACACCACCCCAAATCTGGCTACACACAAACCCCGCTTCCTCC
********                                             P
AAATCTCCTCAGCTGGCGTCCGAAGCCTCCACCCGCCACAGTGAGGCTCG
GATCGTGCCTCCAGAGCGGGTCTCAAACCGCCTACACCAGCTTCCCCGGT
CAACCCCTTCGCAGCGCCGGGAAGTAGCCGAAGGCCTTCGGCAGGTTCCG
CCAGTAGCGCGGGGGCGGGGCCTGTCGAGCGGCTCCGGGTCGAGCTCGGC
TGTTTCCGTGAGTGGCCGCTGCGCACTCGGCACTGGGCGGCGCTGGCTGG
CTCCCTGGCTGCGGCTCCTCAGTCGGCGGCGGCTGCTGCTGCCTGTGGCC
CGGGCGGCTGGGAGAAGCGGAGTGTTGGTGAGTGACGCGGCGGAGGTGTA
GTTTGACGCGGTGTGTTACGTGGGGGAGAGAATAAAACTCCAGCGAGATC
CGGGCCGCGAACGAAAGCAGTGACGGAGGAGCTTGTACCACCGGTAAGAG
GAGCAGGAGGAGGAGGCAGGAGCCGGAGAGAGCCGGGGGGACAGAGGGGG
GCCGGGGAGGCGCCGGACACCCGCGCTCGGGGCCTTCCCCTCGCAGGAGG
      S
GGCCGCGGTAAAGATGGAGCCTCCGCCCGAGCCCCACAACACCGCCGCCG
CTCGCAG
```

```
CONSENSUS SEQUENCES (and reverse complement)
GGGGACTTTCCC -> GGGAAAGTCCCC
GGGGGCTTCCC -> GGGAAGCCCCC
GGGGACCCCC -> GGGGGTCCCC
GGGGAGGGGAATCC -> GGATTCCCCTCCCC
GGGGGCTTTCCC -> GGGAAAGCCCCC
GGGGATTCCC -> GGGAATCCCC
GGGGATCCCC -> GGGGATCCCC (palindrome)

REFERENCES:
FANTOM Consortium: P. Carninci, et al. The transcriptional landscape of the
mammalian genome. Science 309(5740), 1559-63 (2005).
Shiraki, T., et al. Cap analysis gene expression for high-throughput analysis
of transcriptional starting point and identification of promoter usage. Proc
Natl Acad Sci U S A. 100(26), 15776-81 (2003).
LINKS:
      CAGE: http://fantom31p.gsc.riken.jp/cage/mm5/
```

Chromatin Immunoprecipitation (ChIP) protocol

Whole Mouse forebrain was removed from decapitated rats by gross dissection, minced to ~1 mm-sized pieces, and immediately cross-linked in 1% formaldehyde for 15 min at 37C. Adding glycine to a final concentration of 0.125 M stopped the crosslinking reaction. The tissue was washed four to six times in cold PBS containing proteinase inhibitors (1 mM PMSF, 1 µg/ml apoprotinin, and 1 µg/ml pepstatin A) and then frozen on dry ice.

The chromatin was solubilized and extracted by detergent lysis, followed by sonication. First, minced, fixed hippocampal tissue was homogenized twice, for 10 sec, in a cell lysis buffer (10 mM Tris, 10 mM NaCl, and 0.2% NP-40). The homogenate was centrifuged at 5500 x g for 5 min. The supernatant, containing extracellular debris, was decanted, and the pellet was homogenized two more times, for 10 sec, using nuclear lysis buffer (ChIP kit number 17-295; Upstate Biotechnology, Lake Placid, NY). Next, the extracted chromatin was sheared to 400-600 bp using the Sonic Dismembrator 550 (Fisher, Hampton, NH). Each sample was sonicated 120 times on ice, 1 sec each, at 25% of maximum power.

Chromatin immunoprecipitation assays were performed to measure the levels of histone acetylation or phosphoacetylation at various promoter regions. A protocol outlined in the ChIP kit (Upstate Biotechnology) was used, with some modifications. After the chromatin lysate was extracted and properly fragmented to 400-600 bp, the optical density of each sample was determined. Equal amounts of chromatin lysate (60 µg) were diluted with ChIP dilution buffer (kit number 17-295; Upstate Biotechnology) to a final volume of 1.5 ml. One hundred microliters of the pre-immunoprecipitated lysate were saved as "input" for later normalization.

The chromatin solution was pre-cleared with salmon sperm DNA/protein A-agarose 50% gel slurry (catalog #22811; Pierce, Rockford, IL) for 45 min. It was then immunoprecipitated overnight at 4°C with 5 µg of antibody directed against H3 acetylated on Lys9 and Lys14 (kit number 06-599). As a control, samples were immunoprecipitated with 5 µg nonimmune rabbit IgG (kit number 12-370; Upstate Biotechnology). After immunoprecipitation, the DNA-histone complex was collected with 40 µl of salmon sperm DNA/protein A-agarose beads for 2 hr. The beads were sequentially washed once with low salt, high salt, and LiCl and washed twice with 10 mM Tris (pH 8)/1 mM EDTA buffers (kit number 17-295; Upstate Biotechnology). The DNA-histone complex was then eluted from the beads with 500 µl of NaHCO3/SDS elution buffer. DNA and histones were dissociated at 65°C for 4 hr under high-salt conditions. Proteins were digested using proteinase K treatment for 1 hr at 45°C. The DNA, associated with acetylated and phosphoacetylated histones, was extracted with phenol/chloroform/isoamyl alcohol, precipitated with 100% ethanol, and finally resuspended in 80 µl of PCR-grade water. Most ChIP experiments were performed twice, on two independent tissue samples, for confirmation.

Quantification of DNA by real-time PCR. Levels of specific histone modifications at each gene promoter of interest were determined by measuring the amount of acetylated or phosphoacetylated histone-associated DNA by quantitative real-time PCR (BioRad iCycler, BioRad). Specific primers were designed to amplify proximal promoter regions, <200 bp long. For TNFα, the primers 5'-GAGGGGAATCCTTGGAAGAC-3' and 5'-AATTCACGGACCTCACAAGC-3' amplified a region 380 bp upstream of the start codon, which contains a p50-homodimer consensus sequence (GGGGCTTTCC). Input and immunoprecipitated DNA amplification reactions were run in triplicate in the presence of SYBR-Green (Applied Biosystems). Ct values from each sample were obtained. Relative quantification of template was performed as described by the Applied Biosystems manual. Mean and SEM values were determined for each fold difference, and these values were used in two-tailed paired t tests (which were adjusted for multiple comparisons) to determine statistical significance ($p < 0.05$). Each PCR reaction, run in triplicate for each brain sample, was repeated at least two independent times.

References

1. Foster, J. A., Puchowicz, M. J., McIntyre, D. C., & Herkenham, M. (2004) *J Comp Neurol* **476,** 91-102.
2. Kassed, C. A. & Herkenham, M. (2004) *Behav Brain Res* **154,** 577-584.
3. Shumyatsky, G. P., Tsvetkov, E., Malleret, G., Vronskaya, S., Hatton, M., Hampton, L., Battey, J. F., Dulac, C., Kandel, E. R., & Bolshakov, V. Y. (2002) *Cell* **111,** 905-918.
4. Butterweck, V., Winterhoff, H., & Herkenham, M. (2001) *Mol Psychiatry* **6,** 547-564.
5. Guerrini, L., Blasi, F., & Denis-Donini, S. (1995) *Proc Natl Acad Sci U S A* **92,** 9077-9081.
6. Kaltschmidt, C., Kaltschmidt, B., & Baeuerle, P. A. (1995) *Proc Natl Acad Sci U S A* **92,** 9618-9622.
7. Wellmann, H., Kaltschmidt, B., & Kaltschmidt, C. (2001) *J Biol Chem* **276,** 11821-11829.
8. Meffert, M. K., Chang, J. M., Wiltgen, B. J., Fanselow, M. S., & Baltimore, D. (2003) *Nat Neurosci* **6,** 1072-1078.
9. Goslin, K. & Banker, G. (1992) in *Culturing nerve cells*, eds. Banker, G. & Goslin, K. (MIT Press, Cambridge, MA), pp. 252-281.
10. Vermeulen, L., De Wilde, G., Van Damme, P., Vanden Berghe, W., & Haegeman, G. (2003) *Embo J* **22,** 1313-1324.
11. Chen, L. F. & Greene, W. C. (2003) *Journal of molecular medicine (Berlin, Germany)* **81,** 549-557.
12. Vermeulen, L., De Wilde, G., Notebaert, S., Vanden Berghe, W., & Haegeman, G. (2002) *Biochem Pharmacol* **64,** 963-970.
13. Madrid, L. V., Mayo, M. W., Reuther, J. Y., & Baldwin, A. S., Jr. (2001) *J Biol Chem* **276,** 18934-18940.
14. Sizemore, N., Leung, S., & Stark, G. R. (1999) *Mol Cell Biol* **19,** 4798-4805.
15. Schmitz, M. L., Bacher, S., & Kracht, M. (2001) *Trends Biochem Sci* **26,** 186-190.
16. Chen, L. F. & Greene, W. C. (2004) *Nat Rev Mol Cell Biol* **5,** 392-401.
17. Yoshiyama, Y., Arai, K., & Hattori, T. (2001) *Neuroreport* **12,** 2641-2645.
18. Bhakar, A. L., Tannis, L. L., Zeindler, C., Russo, M. P., Jobin, C., Park, D. S., MacPherson, S., & Barker, P. A. (2002) *J Neurosci* **22,** 8466-8475.
19. Zhang, W., Potrovita, I., Tarabin, V., Herrmann, O., Beer, V., Weih, F., Schneider, A., & Schwaninger, M. (2005) *J Cereb Blood Flow Metab* **25,** 30-40.
20. Freudenthal, R., Boccia, M. M., Acosta, G. B., Blake, M. G., Merlo, E., Baratti, C. M., & Romano, A. (2005) *Eur J Neurosci* **21,** 2845-2852.
21. Boccia, M., Freudenthal, R., Blake, M., de la Fuente, V., Acosta, G., Baratti, C., & Romano, A. (2007) *J Neurosci* **27,** 13436-13445.
22. Fridmacher, V., Kaltschmidt, B., Goudeau, B., Ndiaye, D., Rossi, F. M., Pfeiffer, J., Kaltschmidt, C., Israel, A., & Memet, S. (2003) *J Neurosci* **23,** 9403-9408.
23. Hirano, F., Tanaka, H., Hirano, Y., Hiramoto, M., Handa, H., Makino, I., & Scheidereit, C. (1998) *Mol Cell Biol* **18,** 1266-1274.
24. Wang, J. K., Li, T. X., Bai, Y. F., & Lu, Z. H. (2003) *Analytical biochemistry* **316,** 192-201.